TECHNICAL REPORT ARTSD-TR-81005

UNIVERSAL TURRET SYSTEM MODEL DETERMINATION AND CONTROLLER PERFORMANCE TESTING

G. A. STRAHL
R. A. PETERSON

APRIL 1982

US ARMY ARMAMENT RESEARCH AND DEVELOPMENT COMMAND
TECHNICAL SUPPORT DIRECTORATE
DOVER, NEW JERSEY

The views, opinions, and/or findings contained in this report are those of the author and should not be construed as an official Department of the Army position, policy or decision, unless so designated by other documentation.

Destroy this report when no longer needed. Do not return to the originator.

Citation in this report of the names of commercial firms or commercially available products or services does not constitute official endorsement or approval of such commercial firms, products, or services by the US Government.

UNCLASSIFIED

SECURITY CLASSIFICATION OF THIS PAGE (When Data Entered)

REPORT DOCUMENTATION PAGE	READ INSTRUCTIONS BEFORE COMPLETING FORM
1. REPORT NUMBER: Technical Report ARTSD-TR-81005	2. GOVT ACCESSION NO.: AD-A117687
3. RECIPIENT'S CATALOG NUMBER	
4. TITLE (and Subtitle): UNIVERSAL TURRET SYSTEM MODEL DETERMINATION AND CONTROLLER PERFORMANCE TESTING	5. TYPE OF REPORT & PERIOD COVERED: Final, October 1980 - May 1981
	6. PERFORMING ORG. REPORT NUMBER
7. AUTHOR(s): G. A. Strahl, R. A. Peterson	8. CONTRACT OR GRANT NUMBER(s)
9. PERFORMING ORGANIZATION NAME AND ADDRESS: ARRADCOM, TSD, Ware Simulation Section (DRDAR-TSE-SW), Rock Island, IL 61299	10. PROGRAM ELEMENT, PROJECT, TASK AREA & WORK UNIT NUMBERS: AMCMS Code 612617.H190C11
11. CONTROLLING OFFICE NAME AND ADDRESS: ARRADCOM, TSD, STINFO Div (DRDAR-TSS), Dover, NJ 07801	12. REPORT DATE: April 1982
	13. NUMBER OF PAGES: 73
14. MONITORING AGENCY NAME & ADDRESS(if different from Controlling Office): ARRADCOM, TSD, Test and Instrumentation Div (DRDAR-TSE-S), Dover, NJ 07801	15. SECURITY CLASS. (of this report): Unclassified
	15a. DECLASSIFICATION/DOWNGRADING SCHEDULE

16. DISTRIBUTION STATEMENT (of this Report)

Approved for public release; distribution unlimited.

17. DISTRIBUTION STATEMENT (of the abstract entered in Block 20, if different from Report)

18. SUPPLEMENTARY NOTES

19. KEY WORDS (Continue on reverse side if necessary and identify by block number)

Universal turret system
Optimal control
Turret control
Aircraft weapons
Model identification
Bode plots
Weapon dispersion
Statistical analysis

20. ABSTRACT (Continue on reverse side if necessary and identify by block number)

Objectives of the testing were to obtain necessary data to determine a valid mathematical model for a universal turret system and to test the performance of optimal turret controllers designed and built for the UTS using that model.

Two distinct test phases were conducted: the model determination and the controller performance testing. First, the model determination testing is (cont)

DD FORM 1 JAN 73 1473 EDITION OF 1 NOV 65 IS OBSOLETE

UNCLASSIFIED

SECURITY CLASSIFICATION OF THIS PAGE (When Data Entered)

Block 20--Continued

reported, including turret preparation, test plan preparation and modification, and test execution. Then, the optimal controller design and performance testing is covered.

Results of both firing and nonfiring tests are reported and analyzed. The frequency response (Bode) plots are compared to derived theoretical results. The UTS optimal controller performance is compared to the performance of the UTS original controller and of the prototype XM97 controllers tested in a previous program by the use of statistical analysis technique.

CONTENTS

TABLE

FIGURES

INTRODUCTION

This report covers the testing performed on the M97 turret [also known as the Universal Turret System (UTS)] at the Ware Simulation Center (WSC), October 1980 through May 1981, and the improvement in turret performance obtained by implementation of an optimal controller for the turret. Each phase of the testing program is discussed in the report: preparation of the turret, test setup, test plan, and actual testing. Details of the optimal control implementation, a brief interpretation of the test results, and conclusions are presented.

Testing was conducted on the UTS to obtain data necessary to determine validated mathematical models of the azimuth and elevation control systems of the turret. These models will be used to design several optimal controllers for the UTS. One optimal controller has been designed for the UTS with the use of preliminary data. This model was evaluated by nonfiring tests conducted on the turret at WSC. Further optimal controllers will be designed for the UTS once the validated model is determined. These controllers will also be evaluated with test data obtained at WSC. The ultimate goal of the work is to demonstrate the feasibility of designing a controller by use of modern optimal-control-theory techniques to provide improved turret performance over that provided by existing controllers.

BACKGROUND

This work is a continuation of the testing performed during 1979 and 1980 with an early prototype, the XM97 turret. In that program, a mathematical model of the XM97 turret was first experimentally determined. With the model known, modern-control-theory techniques were used to design several optimal controllers for the XM97 turret. These controllers were evaluated by means of firing and nonfiring tests on the XM97 turret at WSC. The test results showed that the optimal controllers provided improved performance over that of the existing conventionally designed controller.

When the improved performance was obtained on the XM97 turret, a decision was made to attempt to extend the results to a production turret. This effort began when a production UTS was obtained and led to the testing described in this report. The testing results provided the necessary information to produce optimally designed controllers for the UTS, which were tested at the WSC.

TURRET DESCRIPTION

The turret tested at WSC is a production model M97 (S/N 1000001) manufactured by General Electric Company. In the field, the UTS is mounted on the AH-1S aircraft and contains the M197 20-mm automatic gun. However, the UTS was designed to be adaptable to a variety of weapons, including the 7.62-mm and 30-mm weapons. The UTS is activated in both azimuth and elevation channels by a controller which employs position, rate, and motor-current feedback to control elec-

tric motors. In addition to the turret motion control circuitry, the UTS contains hardware that handles the weapon fire control.

TEST PROCEDURE

Preparation of Turret

The production model M97 turret and several of its electronic units were used in the test. The Interface Control Unit (IFCU) and several electrical interconnecting harnesses used in the fielded UTS were not available. The available turret electronic units (gun control, logic control, and turret control assemblies) were interconnected in accordance with the UTS interconnection diagram shown on Bell Helicopter drawing number 209-475-049. However, because of the special needs of the test and because no IFCU was available, the procedure involved slight deviation from the drawing. All necessary interconnecting cables were designed and fabricated at WSC. An operational turret suitable for testing was obtained with the use of the available hardware. The UTS turret controller is intact and operational, together with the electrical driving motors in both azimuth and elevation channels. Since no sights or control handles were used, the IFCU was not needed, and the necessary modifications were made to the wiring harness design.

Position commands are input to the elevation and azimuth channels by means of a modified M28 sight simulator (SS) that was connected to the UTS. This SS contains a resolver chain to which the turret resolver chain x-, y-, and z-signals are input. In addition, signals equivalent to gunner position commands, including steps and ramps, are also input to the SS resolver chain. With these inputs, the SS resolver chain transforms the gunner commands into x-, y-, and z-signals, substracts the turret x-, y-, and z-signals, and converts the difference into elevation and azimuth error signals. These error signals are then input to the UTS plant to drive the turret.

The SS also contains system switches that normally would be contained on the pilot's or gunner's control panels, but which are not available on these panels. Included are the turret power, action/standby, and the pilot override switches. A block diagram of the UTS illustrating the main functional units of the system, including the SS, is shown in figure 1. A more detailed drawing of the turret control units is shown in figure 2.

Test Plan

The first phase of the testing was conducted with the UTS mounted on a hardstand. This testing was conducted in accordance with the UTS test plan in appendix A. The second phase involved nonfiring and firing tests conducted with the UTS mounted in a Cobra helicopter on the six-degree-of-freedom (6-DOF) simulator at WSC.

Testing on the hardstand included time and frequency response tests and backlash measurements. Response tests were run with the use of dc, step, ramp, and sinusoidal input signals. Input and response measurements were taken at various places throughout the system (app A). The backlash of the UTS was measured in both the elevation and azimuth channels. The coulomb friction determination and external disturbance tests included in the test plan were not run due to time and equipment limitations. Other deviations from the test plan were found to be necessary due to system nonlinearity.

With the use of preliminary data developed from the above testing, the optimal controller was implemented and tested, together with the original controller, in step tests and firing tests conducted at WSC.

Test Execution

A total of 110 tests were run on the UTS while it was mounted on the hardstand (app B). These tests include step, ramp, dc, and sinusoidal responses. The final two tests run were experimental determinations of the backlash in both the azimuth and the elevation channels.

With some necessary deviations, the step, ramp, dc, and sinusoidal response tests followed the specifications given in the UTS test plan. The deviations were necessary due to system characteristics. One such characteristic was nonlinearity. Analysis of sinusoidal responses taken early in the test indicated that the output was clipped, showing saturation for some inputs. This clipping resulted in reduced gain.

When the input was reduced in those tests where saturation was found, the output was no longer clipped, and a higher gain was observed. Due to this result, the output signal was monitored on an oscilloscope for the remaining sinusoidal response tests. When clipping was seen, the test plan was deviated from and the input was reduced until a linear response was found.

In addition to certain sinusoidal responses, nonlinear characteristics were found in some step responses. The open-loop step responses of the azimuth and elevation forward paths were markedly nonlinear. When the input levels specified in the test plan were used, the output signals were definitely clipped. Therefore the input level was successively halved, with step responses taken each time. Analysis of the output signals indicated that the signals remained clipped for each reduced input but that the source of the clipping came from progressively smaller numbers of saturated operational amplifier stages. When the input was reduced to a level of about ±1 mr, the output finally appeared linearly in both elevation and azimuth.

A second system characteristic requiring test plan deviation was the inability of the signals to be input through the system test points as called for in parts of the test plan. In tests 2, 5, 6, 30, 32, 35, 36, and 60, the test plan calls for the input to be entered through the test points of the UTS turret control assembly (although, for all other tests, the test plan specifies that the input be entered through the sight simulator). When an input is entered through

the test points, only a small portion of the input actually enters the system, due to loading effects. The response received is very small in amplitude and is impossible to analyze. Analysis of the circuitry indicated that considerable modification would have to be made to the test instrumentation to obtain the proper response. Based on this information, a decision was made that the expected data would be insufficient to justify the effort; therefore, the affected tests were dropped.

Other deviations from the test plan were caused by time and equipment considerations. The coulomb friction testing was postponed to a later date due to time restrictions, and the external disturbance tests were delayed until a reliable gyroscope could be obtained. Results from these tests will be included in a later report.

Tests of Original and Optimal Controllers

Following the completion of the tests conducted with the UTS mounted on the hardstand, the turret was put on the Cobra helicopter which was suspended from the 6-DOF simulator at WSC (fig. 3). While mounted in the helicopter, step and firing tests were run on the turret with the use of both the original and an optimal controller.

The optimal controller was designed by Professor N. K. Loh, Oakland University, Rochester, Michigan, by the use of preliminary model data from the WSC testing. Hardware implementation of the design was accomplished by use of the modular turret controller (MTC), a general control system implementation test bed designed and built at WSC.

The optimal controller was designed by the use of modern control theory techniques. The design minimizes a performance index and feeds back certain conditioned state variables to the UTS power amplifier to provide fast, stable control without overshoot (ref 1). Nonfiring and firing tests were run to measure and compare the original and optimal controllers' performance. Step responses with an amplitude of ±5° were run on both systems in azimuth and elevation. In addition, a total of 13 firing tests were conducted by the use of a variety of controller combinations in both channels. A log of the firing tests is shown below:

UTS - modular turret controller firing test log

Test no.	Azimuth controller	Elevation controller
79	Original	Optimal
80	Original	Optimal
81	Optimal	Original
82	Optimal	Original
84	Optimal	Original
85	Original	Original
86	Original	Original
87	Original	Original
94	Optimal	Optimal
95	Optimal	Optimal
96	Optimal	Optimal
97	Optimal	Optimal
98	Optimal	Optimal

DISCUSSION OF RESULTS

This discussion encompasses two main topics. First, the determination of a mathematical model of the UTS (based on the test results) is investigated. Second, the overall system performance is briefly analyzed as the UTS performance is compared with the XM97 turret and with the experimental optimal controllers systems tested at WSC during this and previous programs.

Determination of Mathematical Model

Due to funding limitations, the determination of only a brief portion of the UTS mathematical model was accomplished. The data from all tests performed on the UTS is available at the WSC. This report compares experimental and theoretical results for two circuits of varying complexity. In each case, the experimental results compare closely to the theoretical results. This fact indicates that for the circuits analyzed, the derived theoretical model can be validated as accurate. With additional effort, a validated model for the entire system can be derived.

Experimental results from tests on the demodulator circuits indicate close agreement with theoretical first-order-lag network response. Azimuth demodulator experimental results from test UTS-76 show a flat response out to about 7 hertz, followed by a rolloff which increases to about -20 db/decade above 40 hertz. This curve indicates that the break frequency, the point where the response curve is down 3 db, occurs at 28 hertz. For comparison, a theoretical first-order lag response with a break frequency at 28 hertz is also shown in figure 4. Examination of the azimuth demodulator circuitry indicates that it is a first-order lag with a break frequency of $1/RC = 1/(6.04 \times 10^4 \text{ ohms}) \times (10^{-7} \text{ farads}) =$

166 radians = 26.4 hertz, and has a gain of 5.6 db. Thus, the experimental and theoretical results are in close agreement.

Agreement between experimental results and theoretical prediction is also found for the elevation demodulator circuit. Analysis of the circuitry indicates that the elevation demodulator should demonstrate a first-order lag response with a break frequency = 1/RC = 1/(4.02 X 10^4 ohm) X (10^{-7} farads) = 248.8 radians = 39.6 hertz. Experimental results from test UTS-71 (fig. 5) show a first-order lag magnitude response with a break frequency at 43 hertz.

Phase response for the azimuth demodulator circuit found in test UTS-76 (fig. 6) also indicates agreement with the theoretical predictions. In a first-order lag phase response the break frequency occurs where the phase angle is -45°. The experimental phase response shows the same break frequency of 28 hertz that the magnitude response exhibits.

A more detailed analysis was made on the notch filters used in the UTS because of their complexity. The theoretical transfer function of the notch filter was derived from analysis of the system circuit diagrams. This derivation is shown in appendix C. Once derived, a computer program was used to obtain the gain and phase responses of the theoretical transfer function of the azimuth notch filter. These results are plotted, along with the experimental results from test UTS-15, in figures 7 and 8, and the experimental and theoretical results for the azimuth notch filter compare closely. Similar results can be obtained for the elevation notch filter.

The validity of the transfer functions of the demodulator and the notch filter can be checked by examination of the open-loop test of the forward path up to the notch filter output. This test was UTS-19 for the azimuth channel. If the individual transfer functions are valid and if no interaction exists, the results for test UTS-19 (fig. 9) should be equal to the product of the transfer functions of the demodulator (test UTS-76) and the notch filter (test UTS-15). On the logarithmetic decibel scale, this product is equal to the sum of these two transfer functions. A study of this figure indicates that this product is nearly equal to the sum of the curves of the demodulator in test UTS-76 (fig. 4) and the notch filter in test UTS-15 (fig. 7). The sum of those two curves is also shown in figure 9. This result validates the demodulator and notch filter transfer functions.

Results from other tests listed in the test log can be used to determine the rest of the UTS mathematical model. This same technique of determining individual blocks of the model with appropriate test results and then validating the transfer function with test results of several blocks in series can be applied throughout the UTS model.

System Performance Analysis

In a previous progam conducted at WSC, many of the mathematical model determination tests run on the UTS in this program were performed on the XM97 turret. In both programs (XM97 turret and UTS) following the model determination tests,

new controllers were designed for the turrets by the use of optimal control theory. Each optimal controller was then implemented on the turret and tested.

In both programs, except for the control system electronics, none of the original turret hardware was changed for implementation of the optimal controller; that is, the same motors, gear boxes, power amplifiers, and resolvers were used for both controllers. In the XM97 program, step and firing tests were conducted by the use of the XM97 turret with first its original controller and then the optimal controllers. Details and results of the previous progam will be included in a forthcoming report (ref 2).

Some of the results of that XM97 program are compared to the results of the UTS program in this section. First, a comparison is made of the step responses of the original XM97, original UTS, optimal XM97, and optimal UTS controllers. Also, the backlash of the XM97 and UTS turrets is compared. In addition, the linearity of the two original and the two optimal controllers are analyzed. Finally, the firing test data for each control system is discussed.

Comparison of the step responses indicates that the UTS optimal controller provides the best performance. The measure chosen to judge the performance is the time required for the controller to return to original position (settling time), since this value represents the time required for a control system to return the weapon to the original point-of-aim once it was disturbed. The step responses of the four controllers are shown in figure 10. A comparison of the systems is shown in figure 11. For both the XM97 and the UTS the optimal controller settles to the initial value faster than its counterpart original controller. The UTS optimal controller has a slightly faster settling time than the XM97 optimal controller. The 5% settling times for the four controllers are approximately:

Controller	5% settling time (sec)
XM97 - original	0.68
UTS - original	0.35
XM97 - optimal	0.26
UTS - optimal	0.21

A closer examination of the curves in figures 10 and 11 reveals how the controllers operate and how improved performance is obtained. The original XM97 controller has a long settling time because its initial reaction to disturbance is slow and because it overshoots the original position three times before settling. The original UTS controller obtains a shorter settling time than the original XM97 controller by reacting faster and by reducing the number of overshoots to one. Both optimal controllers obtain faster settling times than the original controllers by eliminating the overshoots. This lack of overshoot is a feature of the optimal design and allows faster, more accurate controllers to be designed.

The UTS exhibited smaller gear backlash than the XM97 turret in both azimuth and elevation. The UTS gear backlash was measured in tests UTS-109 and UTS-110

in accordance with the UTS test plan, whereas the XM97 gear backlash was measured in the same way during a previous program. Backlash values obtained in the testing are:

System	Channel	Backlash (mr)
XM97	Elevation	3.00
XM97	Azimuth	1.40
UTS	Elevation	1.25
UTS	Azimuth	0.84

The UTS controller performs markedly different than the XM97 controller (fig. 10). The UTS reacts more quickly to a disturbance and shows much less overshoot. Part of the reason for this improved performance is due to its reduced backlash, and part is due to certain UTS step and sinusoidal responses. Open-loop step and sinusoidal responses of the UTS forward loop show high gain and nonlinearity.

Similar tests on the XM97 controller in a previous program showed less gain and nonlinearity. In tests UTS-79 through UTS-84, saturation was noted in the output for input levels ranging from ±17 mr to ±2 mr. Saturation was also noted in the forward-loop sinusoidal response test UTS-18. In this test, signals were measured at several locations throughout the system. As the input level was reduced, the output at the end of the forward loop remained saturated, but progressively more stages became unsaturated. Finally, the entire forward path became unsaturated when the input level was reduced to ±20 millivolts. In the sinusoidal responses, saturation has the effect of reducing the gain.

With the nonsaturating input levels in UTS-25, a gain of 60 db was observed. These performances indicate that the UTS has a high forward-loop gain for small input, but this gain is limited for larger inputs due to saturation. Therefore, the UTS can react quickly to disturbances but with less overshoot than the XM97.

Firing Tests

Each firing test considered in this report consisted of bursts (each burst having at least 20 rounds) from the 20-mm M197 gun in conjunction with the XM97 or UTS turret mounted in the Cobra helicopter which was suspended from the 6-DOF simulator at WSC. The M197 used in all firing tests is a three barrel 20-mm gun which fires in a Gatling-gun style. When fired from a hardstand, the M197 produces a firing pattern wherein every round from a given barrel tends to be in general proximity to other rounds from the same barrel (fig. 12). The rounds were color coded so that each target hole could be identified with a round number. Since the M197 is a three-barrel gun, every third round comes from the same barrel (that is, in a 20-round burst, rounds 1, 4, 7, 10, 13, 16, and 19 are from one barrel, rounds 2, 5, 8, 11, 14, 17, and 20 are from the second barrel and rounds 3, 6, 9, 12, 15, and 18 are from the third barrel).

Targets from the XM97 and UTS firing tests also show that rounds fired from the same barrel are in general proximity to each other. In fact, some target patterns approached those shown in the hardstand tests, thus indicating a very good controller. The degree that a test firing pattern resembles that of a hardstand firing pattern is a good indicator of controller performance; therefore, the standard deviation or dispersion of shots from each particular barrel was chosen as a performance measure of the original and optimal controllers.

The impact point of the first round of each barrel in a burst (that is, the first three rounds of a burst) was eliminated from this analysis due to the mechanisms of the helicopter and the finite response time of the controllers. When the M197 gun fires, the recoil force causes the helicopter to pitch quickly downward as shown in figure 13. This pitching motion is so quick that the control system cannot react fast enough to effectively control the first three rounds of a burst. This behavior is very similar for all controllers tested. After the first three rounds, however, the controller can affect the weapon line and can keep the round impact points in fairly close proximity. Since any controller cannot affect the impact points of the first three rounds, these rounds are not included in the controller performance analysis.

The standard deviations of the round impact points for the XM97 and UTS tests (calculated from the round impact points on the target) are shown in appendix D. Units of the numbers were recorded in inches; however, since the range at WSC is 1000 inches long, the numbers also represent milliradians of dispersion. The tests were conducted with the optimal or original system controlling the weapon in azimuth and elevation as indicated. Mean and standard deviations of the standard deviations of the round impact points for bursts obtained with the original and optimal controllers are also shown in appendix D. The most important numbers for analysis of controller performance are the means of the standard deviations for each barrel. They are:

	Standard deviation--means (mr)					
	Barrel 1		Barrel 2		Barrel 3	
Controller	AZ	EL	AZ	EL	AZ	EL
XM97 original	1.25	3.90	1.42	2.73	1.32	2.36
XM97 optimal	1.10	1.98	1.40	2.16	1.35	1.64
UTS original	1.03	1.62	1.34	1.39	0.77	1.65
UTS optimal	0.97	1.53	0.67	1.43	0.64	1.75

Generally the optimal controllers provide smaller dispersion than the original controllers. Also, the UTS with an optimal or original controller has smaller dispersion than the prototype XM97 turret system.

Another method of evaluating the performance of the original and optimal UTS controllers is by comparison of the overall dispersion of their firing patterns. The particular dispersion measure that is used in this report is a determination

of the 80% dispersion circle (that is, the smallest diameter circle that can be drawn on the target that contains 80% of the rounds fired). The radius of that circle is considered the 80% dispersion and the distance, between the center of the circle and the point-of-aim (POA), is considered the 80% mean of the burst or its bias error. This overall dispersion criteria corresponds to a requirement in the Bell Helicopter Development Specification 209-947-281, which states that the UTS shall be capable of firing a 100-round burst so that 80% of the rounds fall within a circle of diameter not greater than 12 milliradians.

Overall 80% dispersion and bias were determined for the UTS firing tests. In addition, they were also found for the weapon hardstand tests that were run to find baseline data for the dispersion of the M197 gun. In this case, the M197 gun was bolted to a rigid mount and test fired. Both 20- and 25-round bursts were shot. The dispersion and bias data for all tests were found manually by use of a template.

Test results are shown in table 1. Overall 80% mean and dispersion data is shown, as well as an indication of which controller was running the azimuth and elevation channels during each UTS test. Mean and dispersion data are in inches of dispersion at the target—which, for the 1000-inch range at WSC, is equivalent to milliradians.

The results shown in table 1 indicate that the optimal controller provides a dispersion that is smaller than that of the original controller and approaches the dispersion from a rigidly mounted M197 gun. Focusing on those tests where the same controller is handling both channels (tests 85 through 87 for the original and tests 94 through 98 for the optimal) and the hardstand tests, the following average dispersions were found:

Test condition	Average 80% dispersion
Turret in helicopter with original controller	3.27 mr
Turret in helicopter with optimal controller	2.74 mr
M197 gun on hardstand	2.31 mr

Controller performance cannot be evaluated by the use of overall dispersion data on those tests where a different controller is used in azimuth and elevation. For those tests, the dispersion in each direction must be taken into account. For this report, it was decided to do the most analysis on individual barrel dispersion data, evaluating dispersion separately in azimuth and elevation for all tests. The individual barrel dispersion is considered to be the best method of analyzing the controller performance with a multibarrel weapon since it reduces the influence of the weapon effect.

Details of a statistical analysis performed on the individual barrel dispersion data are given in appendix D. Basically, the analysis shows that the optimal UTS system provided statistically significant improved performance over the original system in azimuth. In elevation, however, there is no significant dif-

ference between the original and optimal controller's performance. The reverse condition was found for the XM97, where the optimal controller was significantly better than the original controller in elevation, but no significant difference existed in azimuth.

One difference between the XM97 and UTS firing tests is that position gyro feedback was used in elevation for the XM97 test. This position gyro feedback provided a correction for the pitch rotation caused by the weapon recoil force. Gyro feedback was not used in azimuth in the XM97 test and was not used in either channel in the UTS test due to failure of the gyro package. The change in weapon-pointing angle caused by the recoil force is much larger in elevation than in azimuth; and, without elevation gyro feedback, the controller's performance is degraded due to the larger error input. In fact, the larger error input may mask any improvement that would be possible with the UTS optimal controller. In azimuth, with much smaller recoil force, the UTS optimal controller performed much better than the UTS original controller.

The optimal UTS controller was designed very quickly (in less than a week) without knowledge of an accurate mathematical model. Improved performance could be obtained from an optimal controller designed more thoroughly and with the knowledge of an accurate mathematical model. It is quite possible that the model used to design the UTS optimal controller was in more error in elevation than azimuth and that this prevented the UTS optimal controller from being significantly better than the original in elevation as it was in azimuth.

CONCLUSIONS

Two main conclusions are drawn:

1. The performance of the original UTS controller is superior to that of the original XM97 controller.

2. Improved UTS performance is obtained by implementation of an optimal controller.

Also, the following conclusions are drawn:

The original controller and turret of the UTS perform better than the XM97 system did in similar tests. In the original controller, the demodulator produces a much cleaner signal than the XM97. The UTS has a higher forward loop than the XM97, indicating that it can move much faster. This fact is shown in the UTS step responses. Improved controller performance is also demonstrated in the firing tests.

In the turret, the UTS has much smaller gear backlash than the XM97. Since the optimal XM97 turret step response is better than the original UTS step response, an optimal controller can overcome some penalty of gear backlash. If optimal control design techniques are applied to future turret controllers, severe and costly limitations on backlash for the gear train can be relaxed by implementation of proper control algorithms.

An improved UTS turret response was achieved by design of an optimal controller for the system. In the field, the optimal controller could be implemented by simple modification of a few electronic components in the turret control box. It is reasonable to assume that these electronic components could easily fit within the area of components that implement the existing control algorithms. No hardware changes would be required to implement the optimal controller.

All data taken during the tests mentioned in this report is available at WSC for future use. Further information could be obtained by performance of those tests which were listed in the test plan but which were not run due to time and funding limitations. Once all the data was obtained, the entire UTS model could then be validated by applying the procedures used in this report.

REFERENCES

1. N. K. Loh, et al., "Design and Implementation of an Optimal Helicopter Turret Control System," J. of Interdis. Model. and Simul., vol 3, January 1980, pp 31 - 46.

2. N. Coleman, et al., "Application of Modern Control Theory to Design of a Helicopter Turret Control System," ARRADCOM Technical Report, Dover, NJ (to be published).

Table 1. Hardstand firing tests for UTS and M197 automatic gun—80% means and dispersions

Test no.	AZ system	EL system	80% mean (mr)	80% dispersion (mr)
79	Original	Optimal	5.7	3.7
80	Original	Optimal	5.5	2.5
81	Optimal	Original	4.3	2.4
82	Optimal	Original	7.8	2.5
84	Optimal	Original	6.2	3.2
85	Original	Original	5.3	3.0
86	Original	Original	11.0	3.4
87	Original	Original	7.6	3.4
94	Optimal	Optimal	6.7	2.6
95	Optimal	Optimal	7.1	2.6
96	Optimal	Optimal	6.7	2.8
97	Optimal	Optimal	6.2	2.7
98	Optimal	Optimal	6.0	3.0
1*			4.1	2.3
2*			4.3	2.4
3*			5.0	2.0
4*			5.1	2.4
5*			4.4	2.7
6*			4.2	2.1
7*			5.5	2.3

* M197 gun mounted on hardstand.

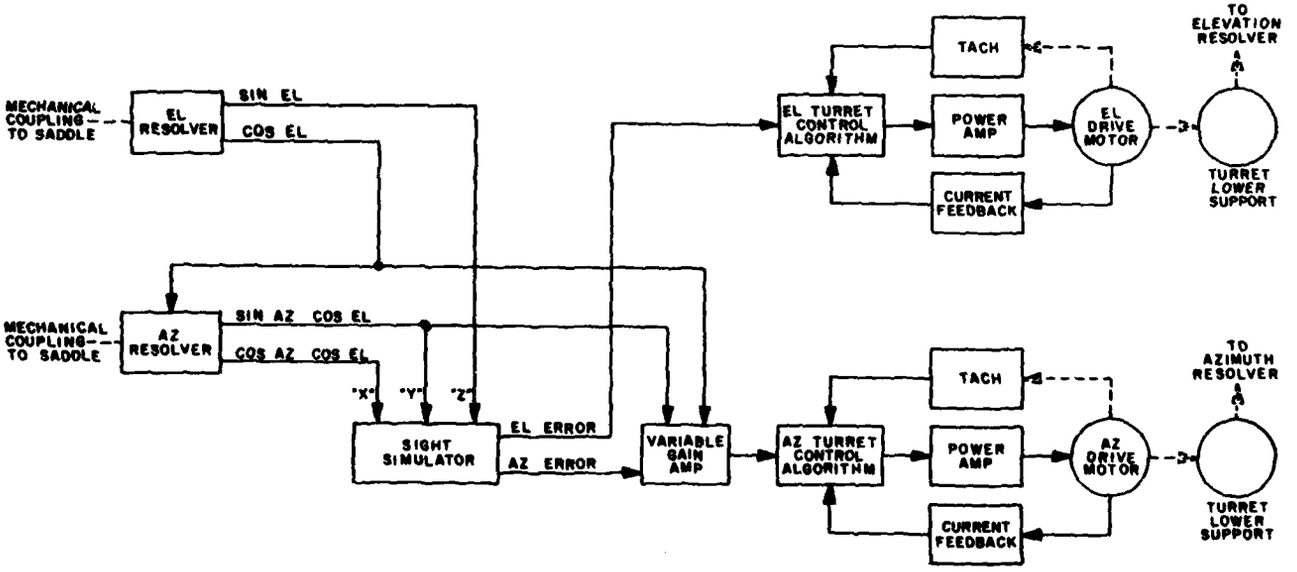

Figure 1. UTS block diagram

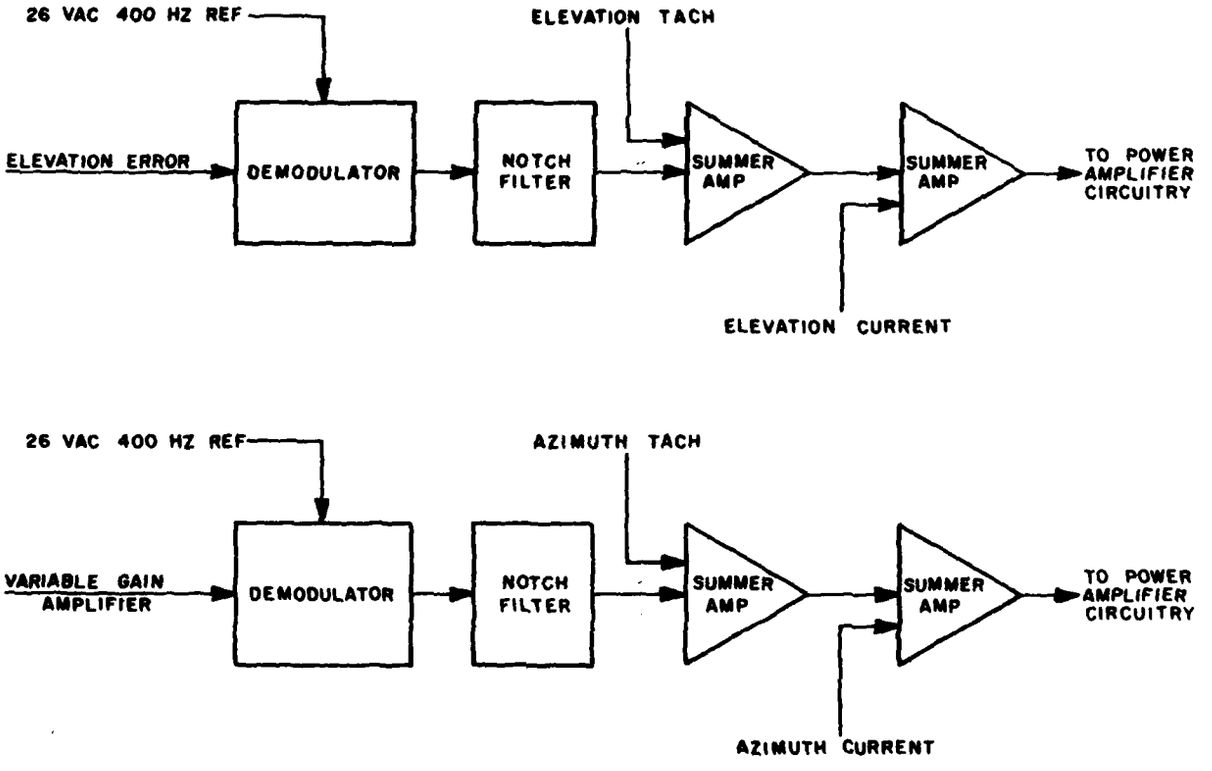

Figure 2. UTS turret control details

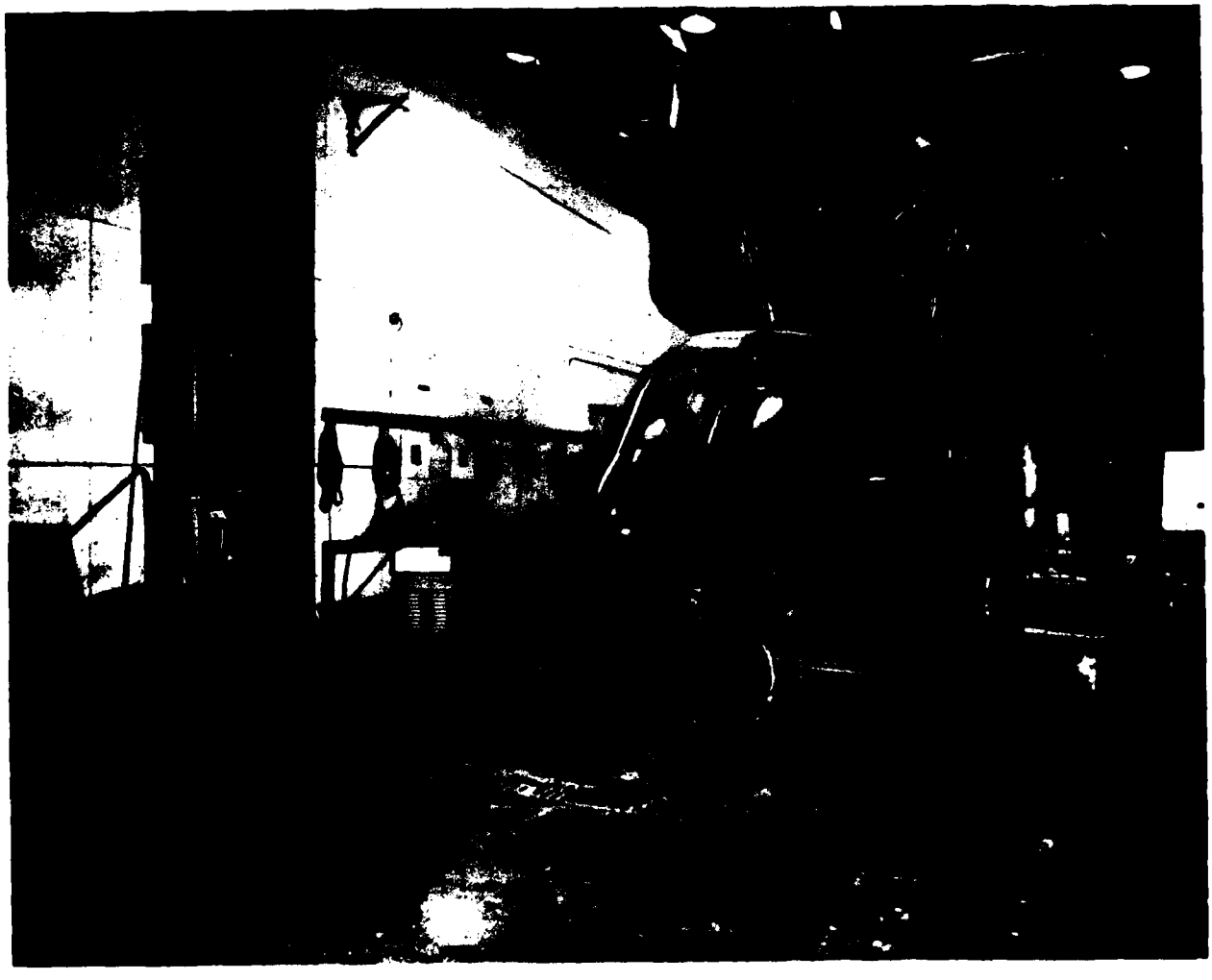

Figure 3. Cobra helicopter suspended from six-degree-of-freedom simulator at Ware Simulation Center

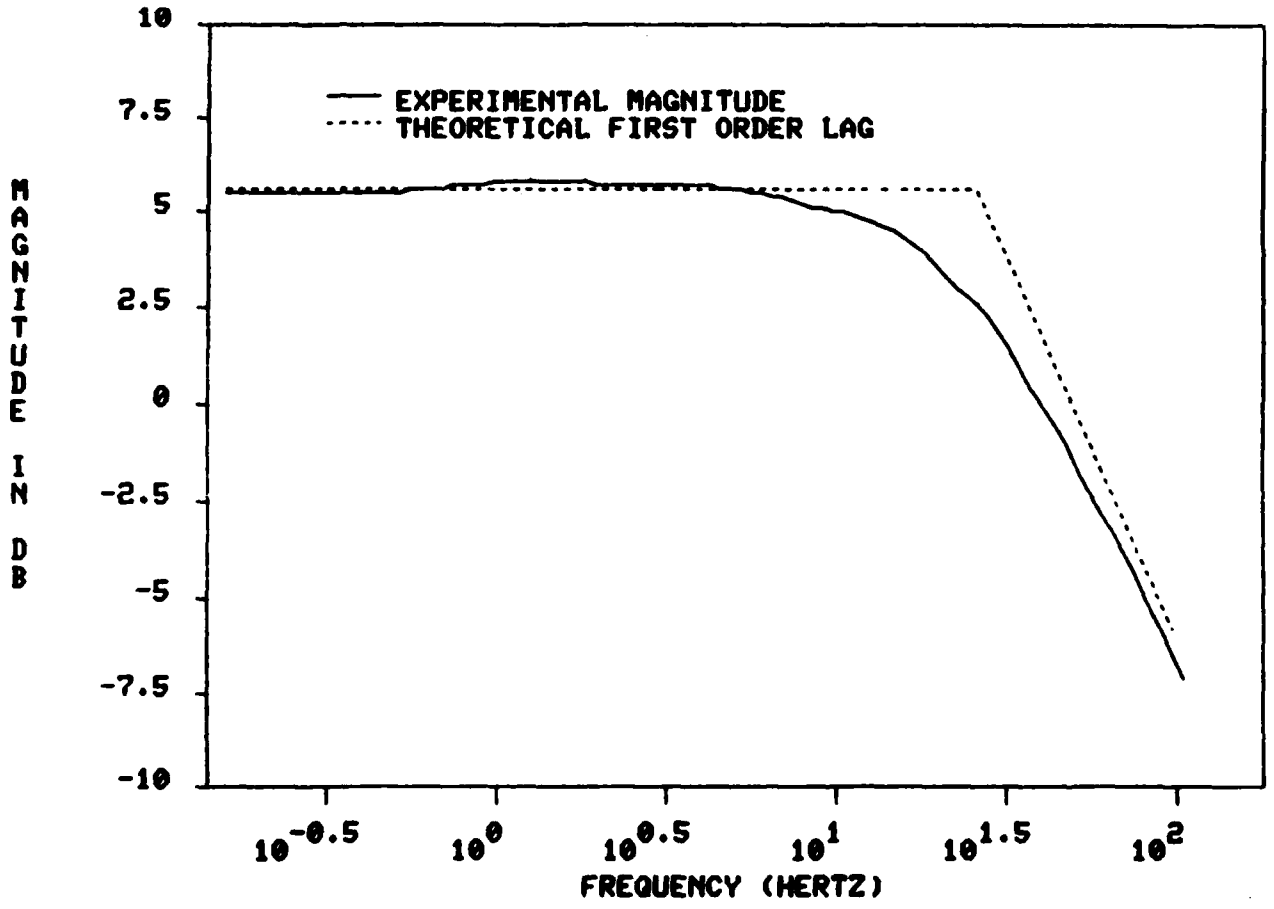

Figure 4. Experimental magnitude and theoretical first-order-lag responses for azimuth demodulator

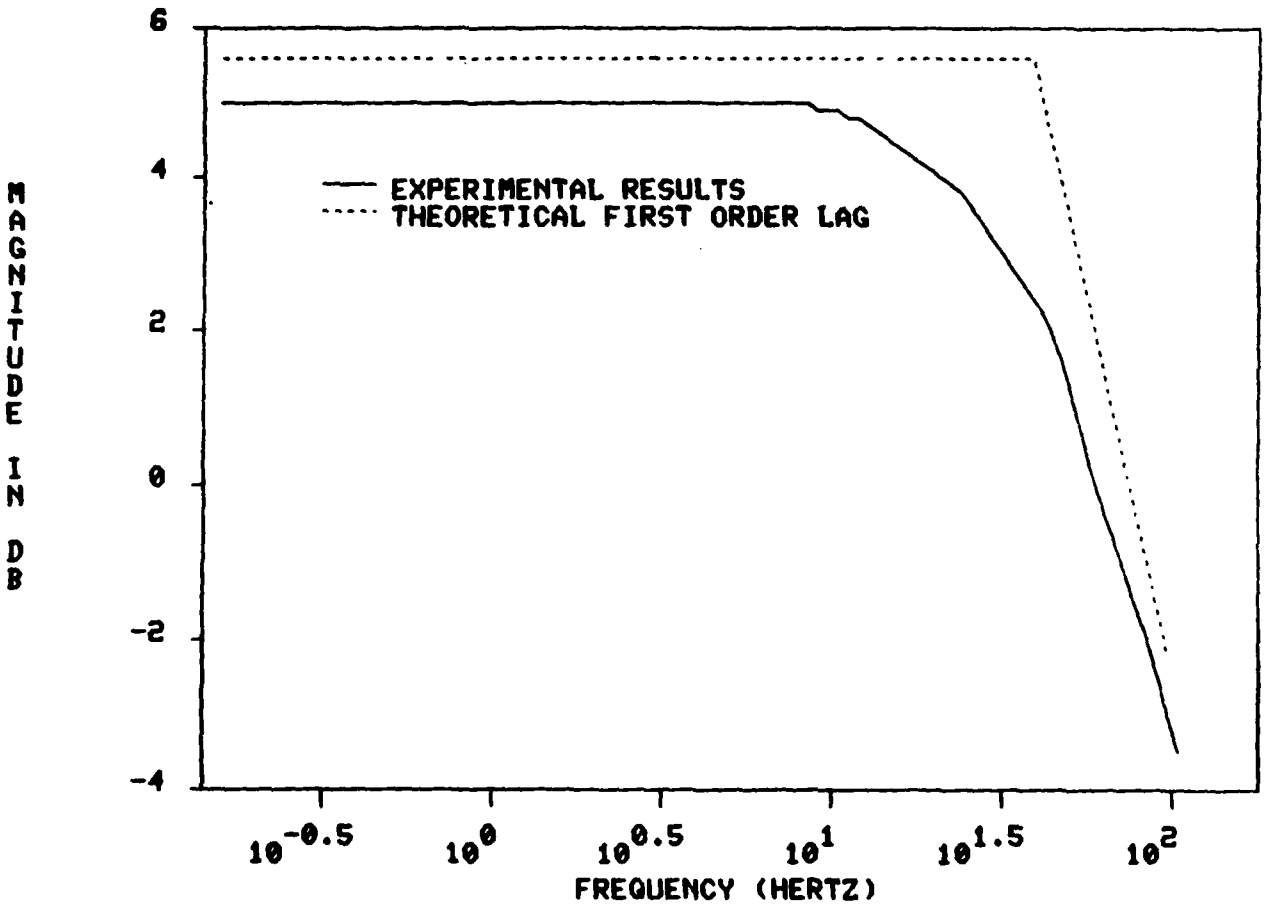

Figure 5. Experimental magnitude and theoretical first-order-lag responses for elevation demodulator

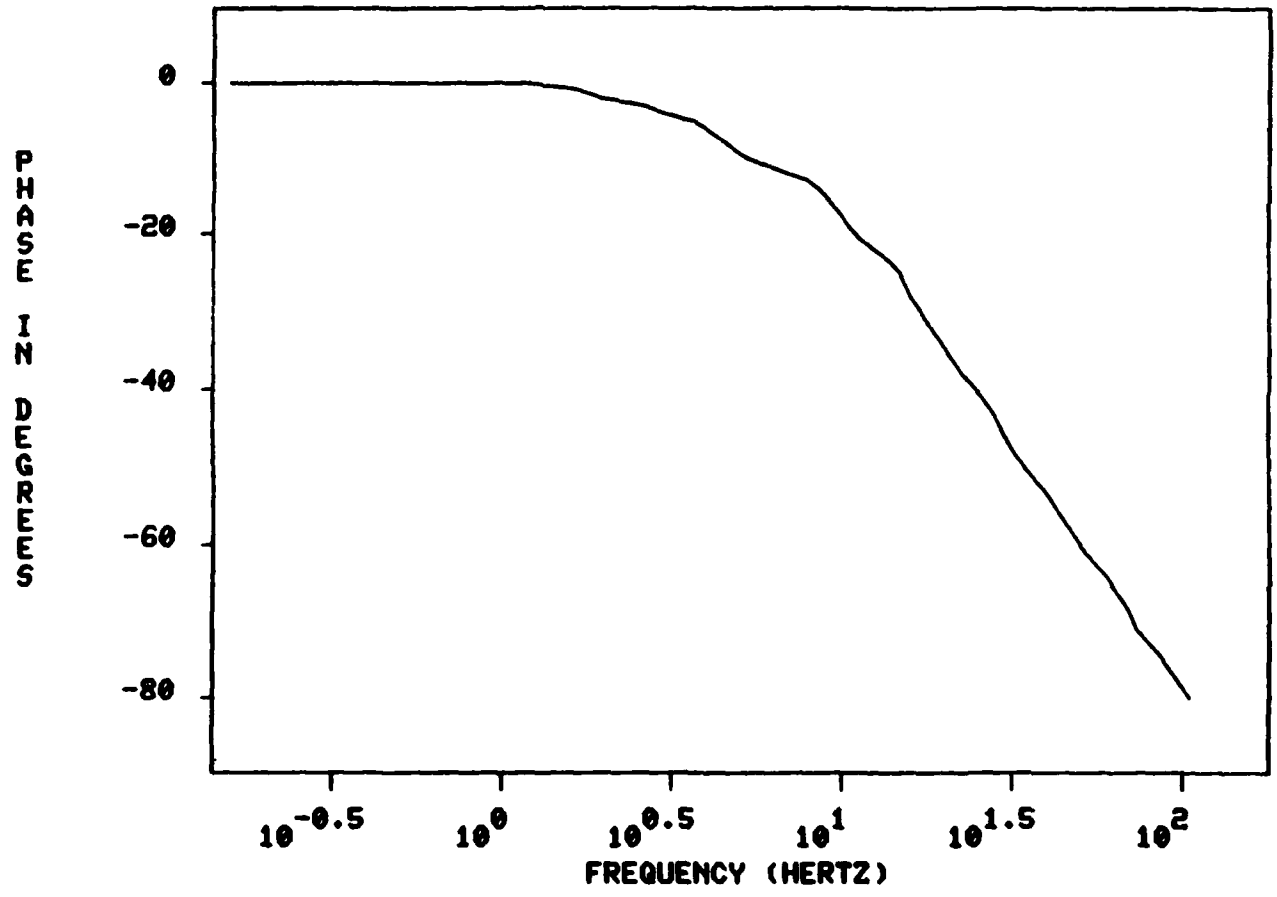

Figure 6. Experimental phase response for azimuth demodulator

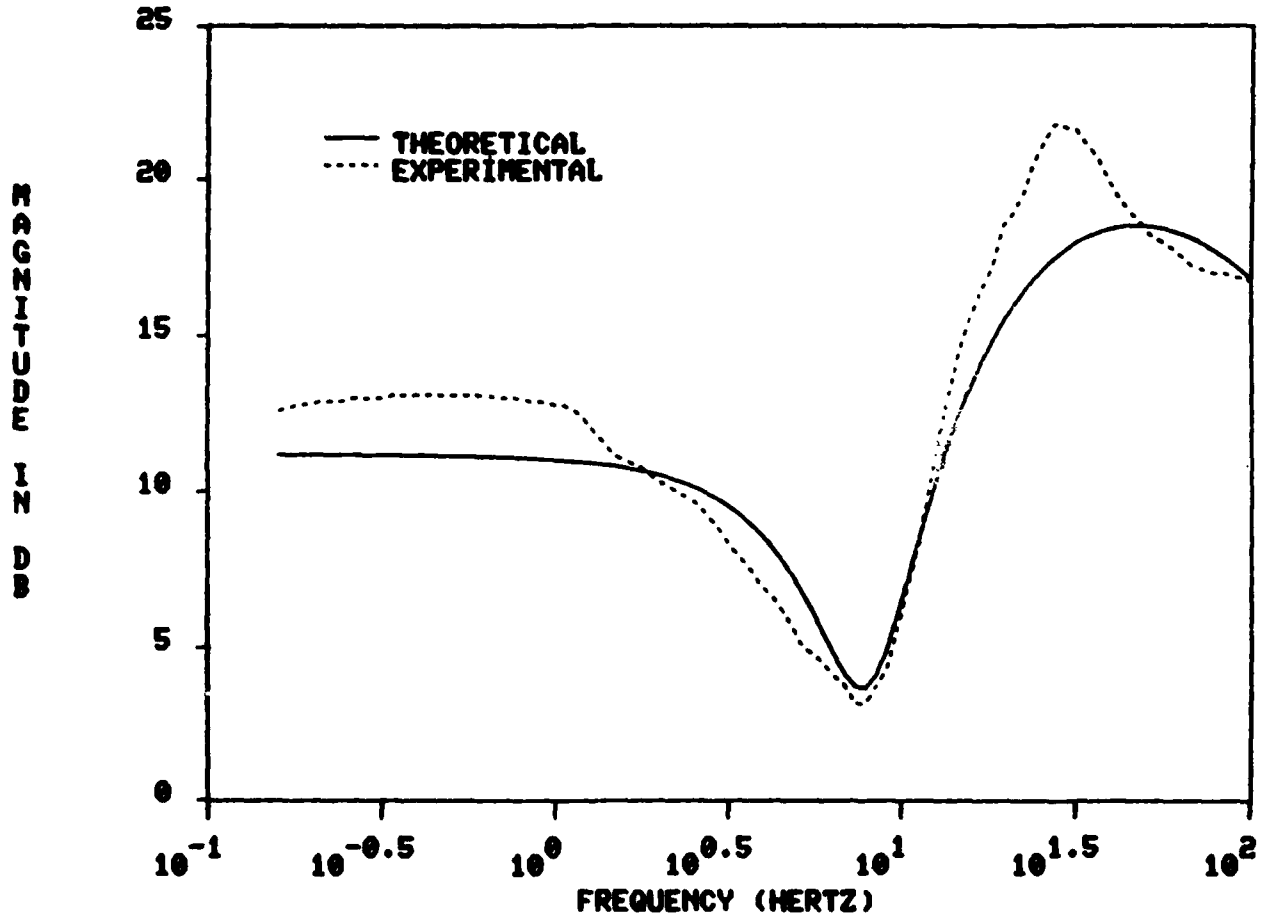

Figure 7. Magnitude transfer functions for azimuth notch filter

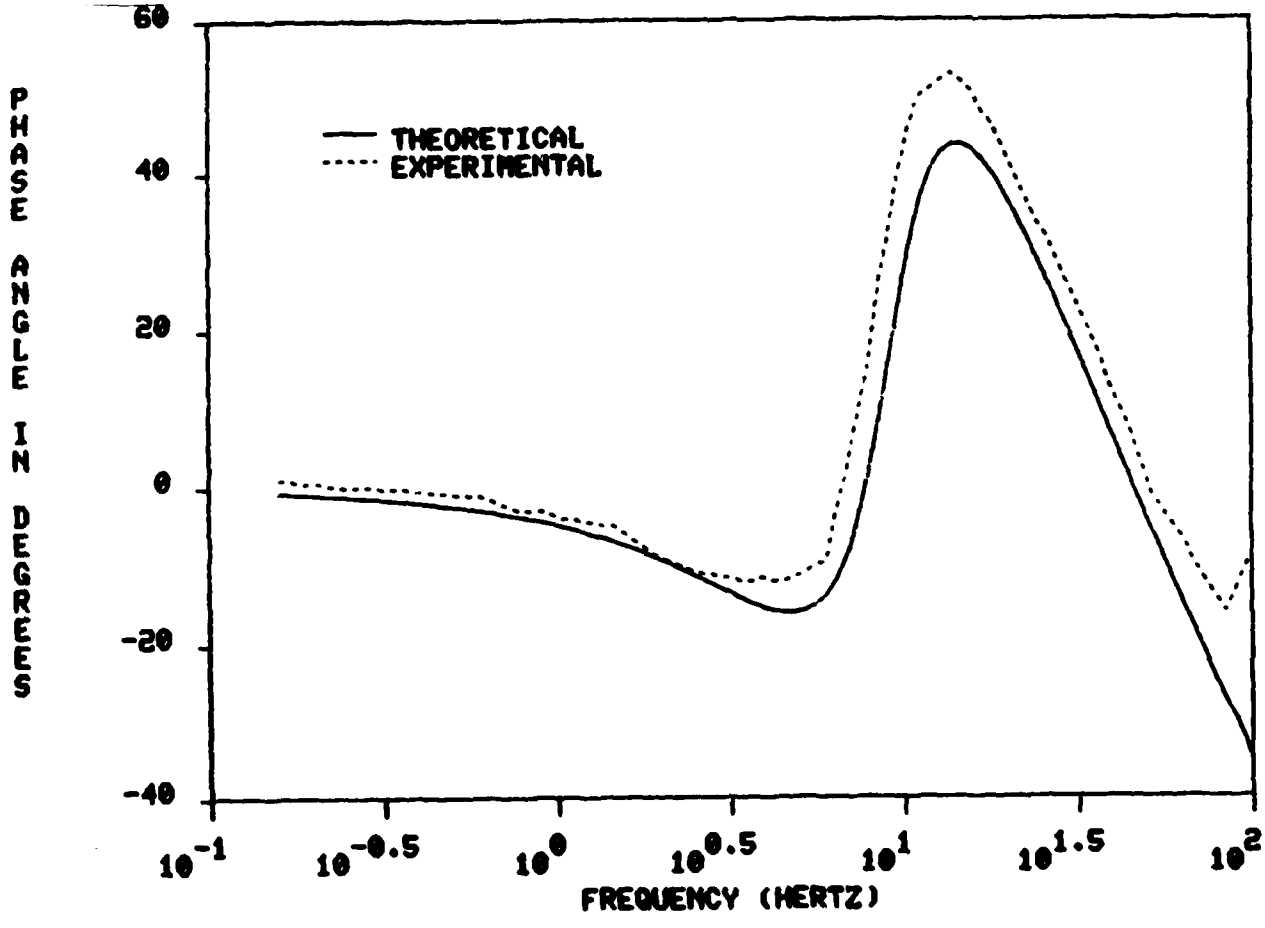

Figure 8. Phase transfer functions for azimuth notch filter

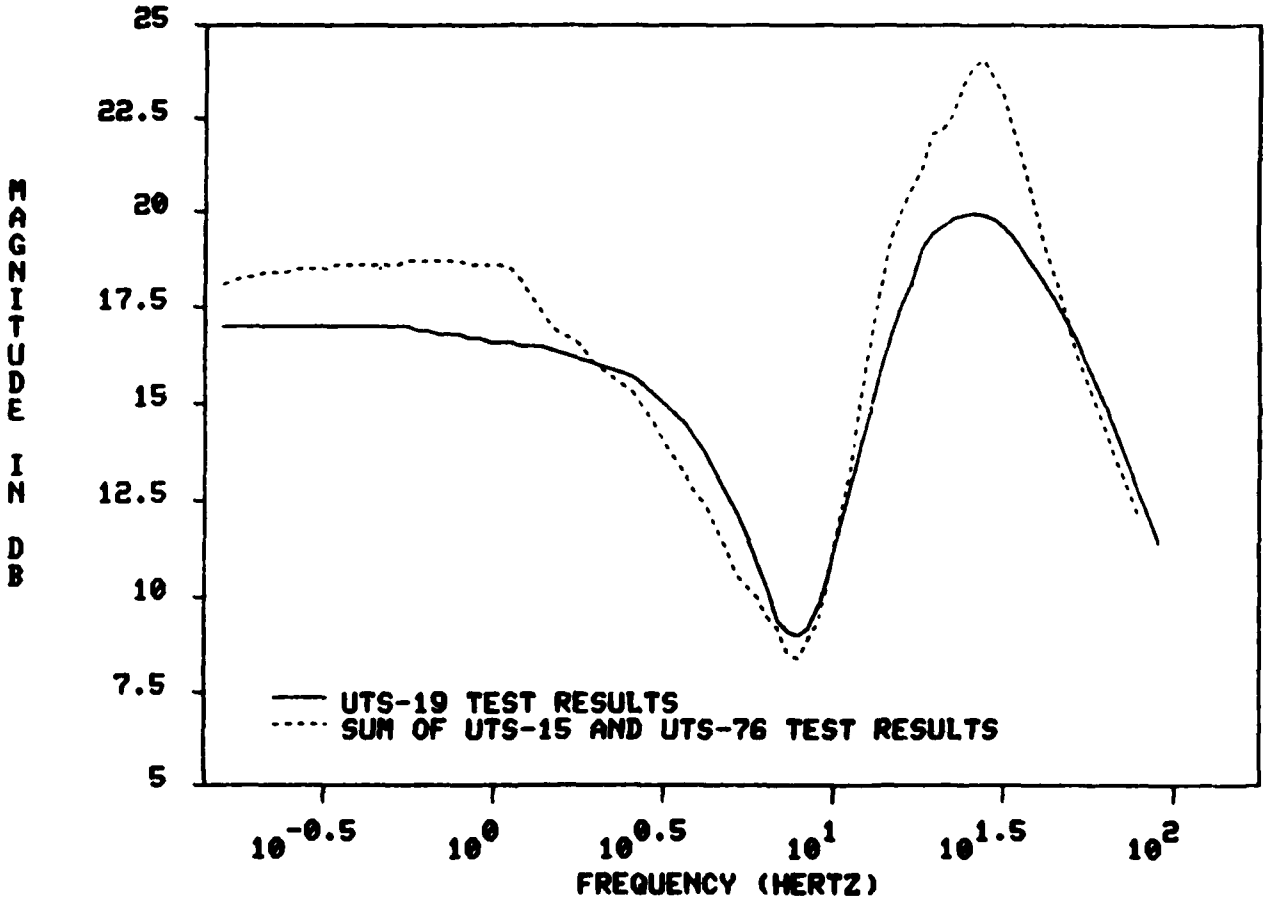

Figure 9. Magnitude response for azimuth demodulator and notch filter

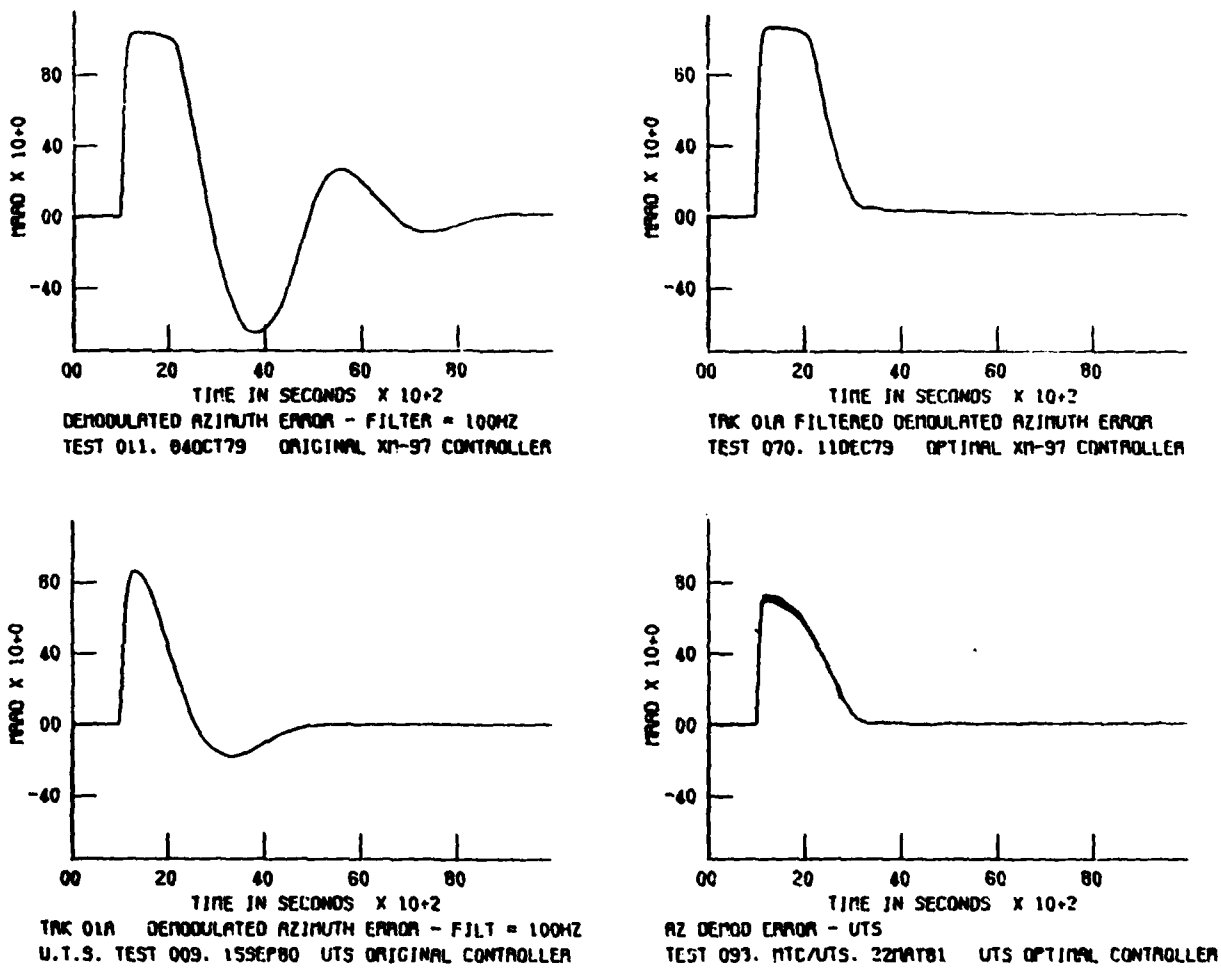

Figure 10. Step responses for UTS original and optimal controllers

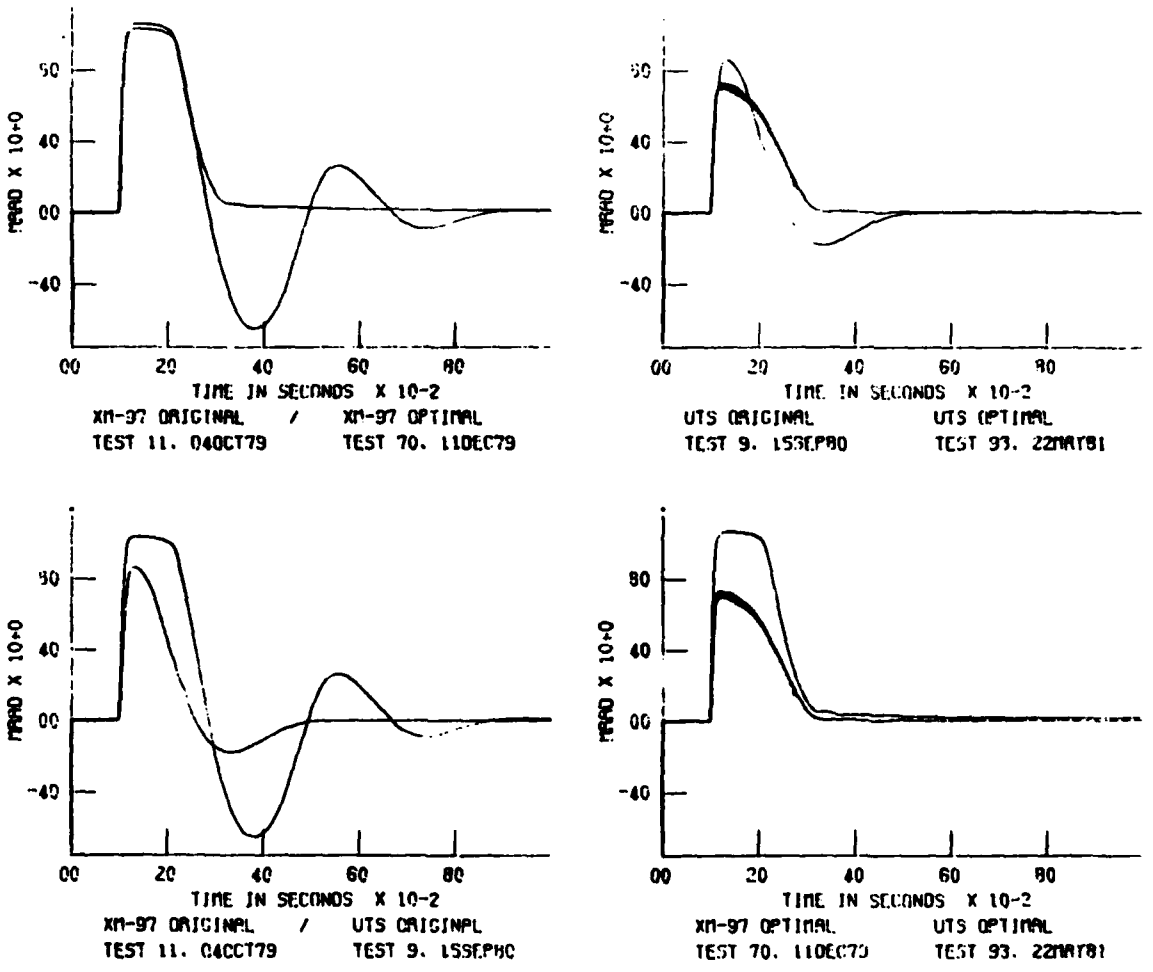

Figure 11. Comparison of step responses for UTS original and optimal controllers

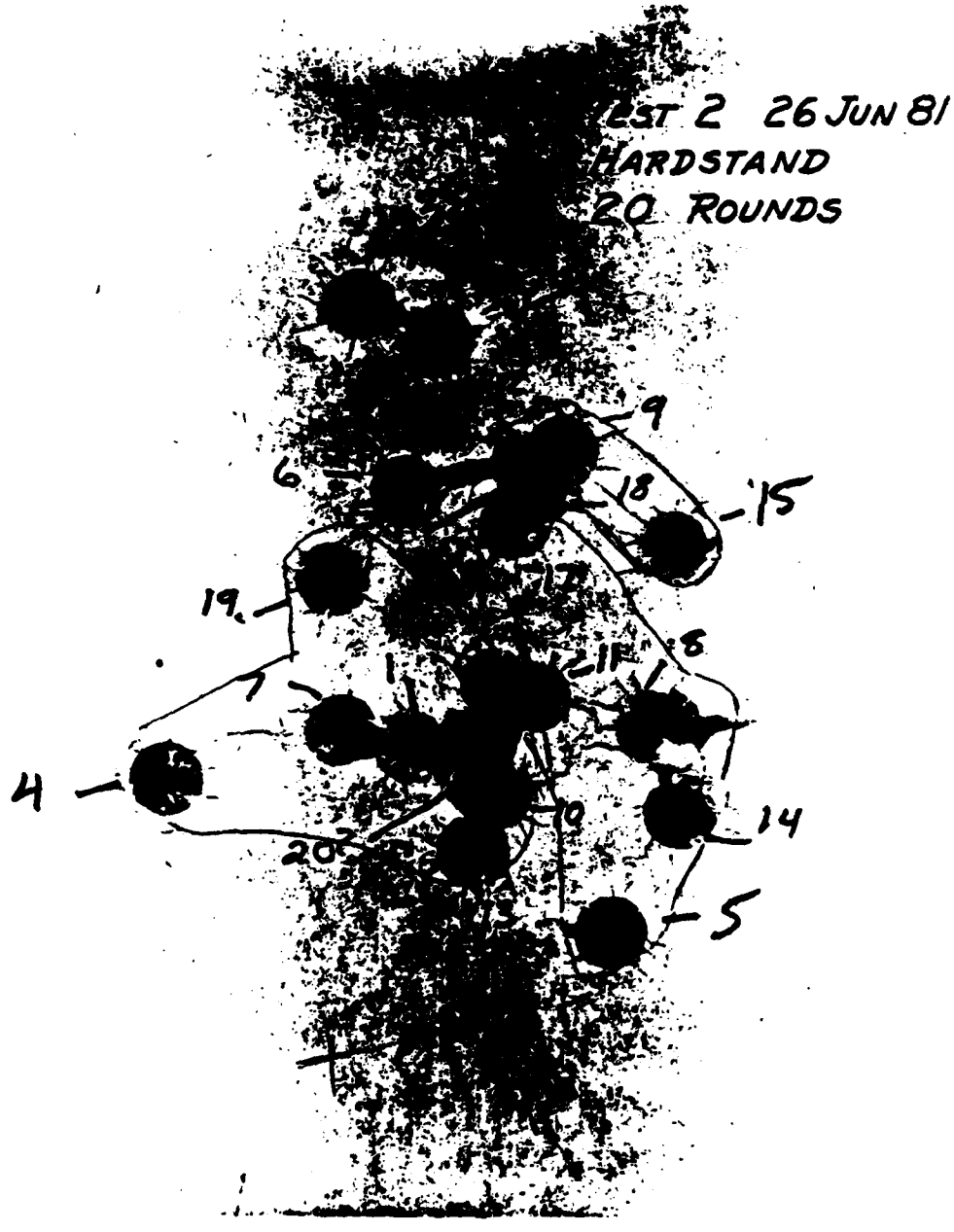

Figure 12. Hardstand firing test pattern of M197 automatic gun

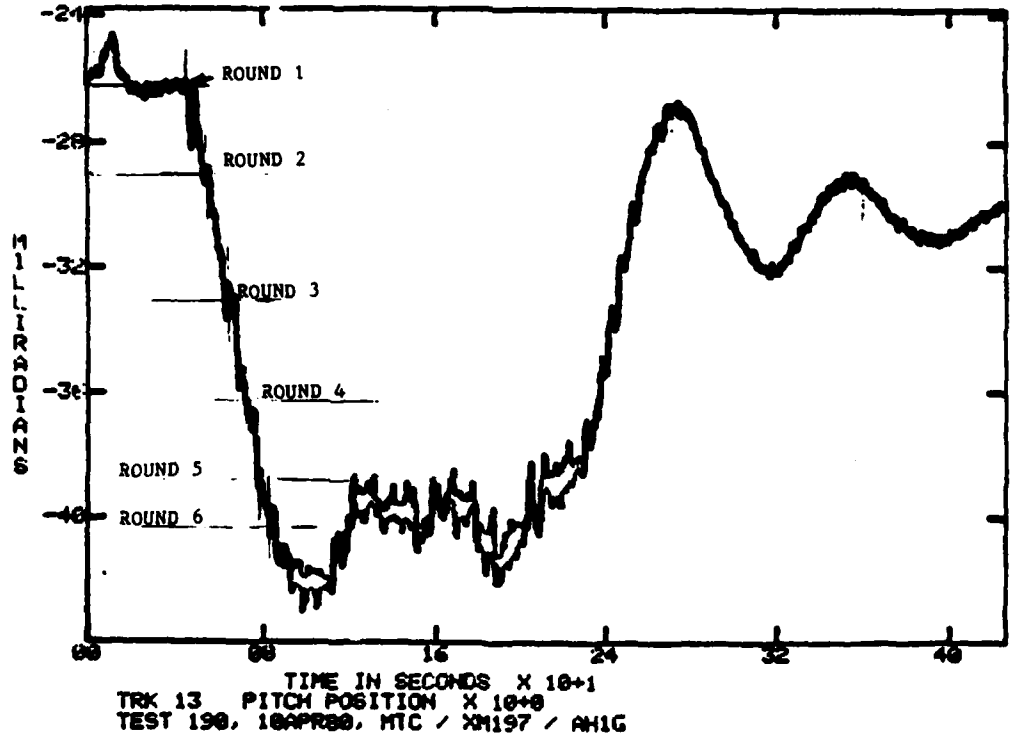

Figure 13. Pitch position of M197 automatic gun during firing test

APPENDIX A

UNIVERSAL TURRET SYSTEM (UTS) TEST PLAN

1. Introduction

The purpose of this test is to establish the values of the system parameters that will be used in future design work in the UTS Program. The majority of the testing will be performed with the UTS mounted on a hard stand. There step, DC, and sinusoidal UTS responses will be measured that will be used to determine system transfer functions and parameters. The UTS backlash and coulomb friction will also be measured. The UTS will also be mounted on the helicopter and subjected to external disturbances from the 6-DOF simulator to determine the system sensitivities to this input.

2. Test Procedure

2.1 DC, Step, and Sinusoidal Response Tests.

2.1.1 UTS step, DC, and sinusoidal responses are to be taken at the Ware Simulation Center. Both open loop and closed loop tests will be made. The test signals will be input and the output response measured at various system points. The frequency response tests will be made using the BAFCO servo-analyzer.

2.1.2 The details of the DC, step, and sinusoidal response tests are given in Figure 1. This figure states the input points, drive signals, and test measurements for each of the tests. For each open loop test, the figure lists what part of the UTS is to be disconnected. The figure identifies what information for each test is to taken on the analog recorder and on channels 1 and 2 of the BAFCO servo-analyzer. The input and tests points mentioned in table A-1 are identified and located in table A-2. All of the points are available either at the sight simulator or the turret control assembly.

2.1.3 The tests listed in table A-1 were devised with the assumption that all disconnections and test measurements listed can be accomplished without damaging UTS components. Each test will be attempted as it is stated in this test plan. If a test cannot be done due to an inability to measure a test point or to run the UTS in a certain configuration, the test will be accomplished while adhering as closely as possible to the test plan.

2.1.4 There is a possibility that time and money constraints will limit the amount of the testing in this plan that may be conducted. If this happens, priority will be given to conducting the elevation tests and those azimuth tests whose results are considered essential in determining a good model. The azimuth tests which are considered essential are marked with an asterisk in table A-1.

2.2 Backlash Measurement.

A backlash measurement of the UTS is to be taken while the UTS is mounted on the hardstand . The backlash will be measured by finding how far the weapon can be turned before engaging gear teeth in both elevation and azimuth by pulling manually on the end of the weapon with no turret power applied. The amount of this turning is equal to the backlash and will be measured using a dial indicator. The backlash measurement will be taken at least eight times in each axis. A mean and standard deviation will be calculated from the data to determine a statistical value for the backlash in elevation and azimuth.

2.3 Coulomb Friction Measurement.

2.3.1 General

The coulomb friction of the UTS will be measured with the turret mounted in the hardstand . The test will consist of a breakaway test and a motor current versus weapon velocity determination.

The weapon velocity will be measured with the UTS tachometer. The motor constants, R, L, K_V, and K_T, and the viscous friction, B, which are needed along with the test data to calculate the coulomb friction,will be taken from the UTS

mathematical model.

Each test will be performed separately in the elevation and azimuth axes.

2.3.2 Breakaway Test.

A force will be applied to the weapon barrels and measured with a dynometer. The force will be increased until the barrels begin to move. This force will equal the static friction. The test will be repeated at least eight times in each axis to obtain a good statistical basis for determining the static friction.

2.3.3 Weapon Velocity Versus Motor Current Determination.

Ramp inputs of various levels will be input to the sight simulator to create different levels of weapon velocity. The test will be conducted in both elevation and azimuth. The input level will be made sufficiently large to reduce the effects of backlash and determine the nonlinear functional characteristics of the coulomb friction.

The weapon velocity and motor current will be measured for each input level. The weapon velocity will be measured using the UTS tachometer.

The coulomb friction will be calculated using the test data and the values given for motor constants given in the UTS mathematical model. The value of backlash determined in the test described in paragraph 2.3.2 will also be used.

2.4 External Disturbance Tests.

2.4.1 The UTS will be mounted on the helicopter on the 6-Degree-Of-Freedom (6-DOF) Simulator. The simulator will be used to impart external motion to the turret. The external motion will be applied in both pitch and yaw axes if a working position gyro can be made operational in each axis within the testing timeframe.

2.4.2 External motion in pitch, and, if possible, yaw, will be applied at the maximum practical amplitude at 0.5, 1.0, and 2.0 hertz. The following measurements

will be taken with external motion applied and turret power operational.

a. Hull position

b. Hull rate

c. Error signal

d. Tachometer signal (weapon velocity)

e. Saddle acceleration

f. Barrel velocity

g. Barrell acceleration

2.4.3 Vertical motion at frequencies of 6.0, 8.5, and 10 hertz will be applied to the UTS turret through the 6-DOF actuators. The amplitude will be the maximum practical to use at the given frequency. The same measurements listed in paragraph 2.4.2 will be taken for this test although the chief interest will be in the barrel and saddle acceleration and barrel velocity to determine barrel motion at these frequencies.

Table A-1. STS System Tests

* Tests Essential to Determine Model (See Paragraph 2.1.4)

TEST NAME	TEST NO.	Input Point (See Fig 5)	Test Point Measurements (See Figure 2) BAPCO Ch. 4	BAPCO Ch. 8	Analog Recorder	DRIVE SIGNAL		DISCONNECT		DESCRIPTION	
* As DC Gain	1	3	-	-	3, 5, 7, 11, 13	400Hz Mod Equiv to 2.0VDC		Azimuth Motor		As DC Open Loop Gain, Input to Demod	
As DC Gain	2	11	-	-	13	2.0 VDC		Azimuth Motor		As DC Open Loop Gain, Input to Amplifier	
* As Step Response	3	1	-	-	All As Channels	1°step,	0.5Hz	As Tach & Pos Fdbk		As Sys Open Loop Step Response	
As Step Response	4	1	-	-	1, 3, 5, 7, 11, 13	1°step,	0.5Hz	Azimuth Motor		As Open Loop Step Res. Motor Disconn.	
As Step Response	5	3	-	-	7, 11,13	1°step,	0.5Hz	Azimuth Motor		As O/L Step Res. Input to Notch Filt	
As Step Response	6	11	-	-	13	1°step,	0.5Hz	Azimuth Motor		As O/L Step Res. Input to Amplifier	
* As Sinusoidal Res	7	1	1	19	-	1° sin,	0.1 - 100 Hz	As Tach & Pos Fdbk		As O/L Sin Res. Forward Path	
As Sinusoidal Res	8	1	1	13	-	1° sin,	0.1-100 Hz	Azimuth Motor		As O/L Sin Res. Forward Path to Motor	
As Sinusoidal Res	9	1	1	7	-	1° sin,	0.1-100 Hz	Azimuth Motor		As O/L Sin Res. thru Notch Filt	
* As Sinusoidal Res	10	1	5	7	-	1° sin,	0.1-100 Hz	Azimuth Motor		As O/L Sin Res. Notch Filt	
* As Sinusoidal Res	11	1	11	13	-	1° sin,	0.1-100 Hz	Azimuth Motor		As O/L Sin Res. Current Loop Amplifier	
As Sinusoidal Res	12	1	9	11	-	1° sin,	0.1-100 Hz	As Tach & Pos Fdbk		As O/L Sin Res. Current Loop, 1/10°ct.	
* As Sinusoidal Res	13	1	18	19	-	1° sin,	0.1-100 Hz	As Tach & Pos Fdbk		As O/L Sin Res. Motor Loop Fwd Path	
As Sinusoidal Res	14	1	1	13	-	1° sin,	0.1-100 Hz	As Tach & Pos Fdbk		As O/L Sin Res. Sight to Current Output	
As Sinusoidal Res	15	1	7	19	-	1° sin,	0.1-100 Hz	As Tach & Pos Fdbk		As O/L Sin Res. Forward Path to Tach	
As Sinusoidal Res	16	1	2	9	-	1° sin,	0.1-100 Hz	As Pos Fdbk		As O/L Sin Res. Rate Loop, 1/10°ct.	
As Open Loop Res	17	1	-	-	19	2.5Hz step amp. for reaction		As Tach & Pos Fdbk		As Open Loop Res. Min Input for Motion	
As Open Loop Res	18	1	-	-	19	2.5Hz step amp. 0.1RAD		As Tach & Pos Fdbk		As Open Loop Res. 0.1 Radian Input	
As Step Response	19	1	-	-	All As Channels	1°step,	0.5Hz	----------		As Closed Loop Step Response, 1° Input	
As Step Response	20	1	-	-	All As Channels	2.5°step,	0.5Hz	----------		As Closed Loop Step Response, 2.5° Input	
* As Sinusoidal Res	21	1	1	3	-	1° & 2.5° sin, 0.1-100 Hz		----------		As Closed Loop Sys Sin Response	
As Sinusoidal Res	22	1	1	19	-	1° & 2.5° sin 0.1 - 100 Hz		----------		As C/L Sin Res, Forward Path	
As Sinusoidal Res	23	1	11	3	-	1° & 2.5° sin 0.1 - 100 Hz		----------		As C/L Sin Res, Torq. Dis. Sim.	
As Sinusoidal Res	24	1	11	19	-	1° & 2.5° sin 0.1 - 100 Hz		----------		As C/L Sin Res, Torq Dis Sig & Filter	
As Sinusoidal Res	25	1	11	19	-	1° & 2.5° Sin 0.1 - 100 Hz		----------		As C/L Sin Res, Torq Dis Forward Path	
As Sinusoidal Res	26	1	1	11	-	1° Sin, 0.1 - 100Hz		As Tach & Pos Fdbk		As O/L Sin Res, Sight to Current Error	
As Sinusoidal Res	27	1	1	9	-	1° Sin, 0.1 - 100Hz		As Tach & Pos Fdbk		As O/L Sin Res, Sight to Rate Loop Error	
As Sinusoidal Res	28	1	1	5	-	1° Sin, 0.1 - 100Hz		As Tach & Pos Fdbk		As O/L Sin Res, Demodulator	
As Sinusoidal Res	29	1	9	13	-	1° Sin, 0.1-100Hz		As Tach & Pos Fdbk		As O/L Sin Res, Rate & Current Loops	
As DC Gain	30	1	-	-	5, 7, 11, 13	2.0 VDC		As Motor		As Open Loop Gain, Input to Filter	

Table A-1. (cont)

TEST NAME	TEST NO.	Input Point (See Fig 1)	Test Point Measurements (See Figure 2) BAPCO Ch. 1	BAPCO Ch. 2	ANALOG	DRIVE	SIGNAL	DISCONNECT	DESCRIPTION
EL DC Gain	31	4	-	-	4,6,8, 12,14	400Hz Mod to 2.0VDC	Equiv	Elevation Motor	EL DC Open Loop Gain, Input to Demod
EL Dc Gain	33	12	-	-	14	2.0VDC		Elevation Motor	EL DC Open Loop Gain, Input to Amplifier
EL Step Response	33	2	-	-	All EL Channels	1°step,	0.5Hz	EL Tach/Pos Fdbk	EL Sys Open Loop Step Response
EL Step Response	34	2	-	-	2,4,6,8, 12,14	1°step,	0.5Hz	Elevation Motor	EL Open Loop Step Res., Motor Discon.
EL Step Response	35	6	-	-	8,12,14	1°step,	0.5Hz	Elevation Motor	EL O/L Step Res., Input to Notch Filt
EL Step Response	36	12	-	-	14	1°step,	0.5Hz	Elevation Motor	EL O/L Step Res., Input to Amplifier
EL Sinusoidal Res	37	2	2	20	-	1°sin,	0.1-100Hz	EL Tach/Pos Fdbk	EL Open Loop Sinusoidal Res., Forward Path
EL Sinusoidal Res	38	2	2	14	-	1°sin,	0.1-100Hz	Elevation Motor	EL O/L Sin Res., Forward Path to Motor
EL Sinusoidal Res	39	2	2	8	-	1°sin,	0.1-100Hz	Elevation Motor	EL O/L Sin Res., Through Notch Filt
EL Sinusoidal Res	40	2	4	8	-	1°sin,	0.1-100Hz	Elevation Motor	EL O/L Sin Res., Notch Filt
EL Sinusoidal Res	41	2	12	14	-	1°sin,	0.1-100Hz	Elevation Motor	EL O/L Sin Res., Current Loop Amplifier
EL Sinusoidal Res	42	2	10	12	-	1°sin,	0.1-100Hz	EL Tach/Pos Fdbk	EL O/L Sin Res., Current Loop, 1/1°sec
EL Sinusoidal Res	43	2	14	20	-	1°sin,	0.1-100Hz	EL Tach/Pos Fdbk	EL O/L Sin Res., Current Loop Fwd Path
EL Sinusoidal Res	44	2	2	14	-	1°sin,	0.1-100Hz	EL Tach/Pos Fdbk	EL O/L Sin Res., Motor Impedance
EL Sinusoidal Res	45	2	8	20	-	1°sin,	0.1-100Hz	EL Tach/Pos Fdbk	EL O/L Sin. Res., Forward Path to Tach
EL Sinusoidal Res	46	2	8	10	-	1°sin,	0.1-100Hz	EL Pos Fdbk	EL O/L Sin. Res., Rate Loop, 1/1°sec
EL Open Loop Res	47	2	-	-	20	2.5Hz Step Min. Amp. for Motion		EL Tach/Pos Fdbk	EL Open Loop Res., Min Input for Motion
EL Open Loop Res	48	2	-	-	20	2.5Hz Step Amp. 0.1Rad.		EL Tach/Pos Fdbk	EL Open Loop Res., 0.1 Radian Input
EL Step Response	49	2	-	-	All EL Channels	1°step,	0.5Hz	----------	EL Closed Loop Step Response, 1° Input
EL Step Response	50	2	-	-	All EL Channels	2.5°step	0.5Hz	----------	EL Closed Loop Step Response, 2.5° Input
EL Sinusoidal Res	51	2	2	4	-	1° & 2.5° Sin 0.1 - 100Hz		----------	EL Closed Loop System Sin Response
EL Sinusoidal Res	52	2	2	20	-	1° & 2.5° Sin 0.1 - 100Hz		----------	EL C/L Sin Res. Forward Path
EL Sinusoidal Res	53	2	12	4	-	1° & 2.5° Sin 0.1 - 100Hz		----------	EL C/L Sin Res. Torque Dist Sin
EL Sinusoidal Res	54	2	12	8	-	1° & 2.5° Sin 0.1 - 100Hz		----------	EL C/L Sin Res. Torque Dist Sin and Filter
EL Sinusoidal Res	55	2	12	20	-	1° & 2.5° Sin 0.1 - 100Hz		----------	EL C/L Sin Res. Torque Dist Forward Path
EL Sinusoidal Res	56	2	2	12	-	1° sin,	0.1 - 100Hz	EL Tach & Pos Fdbk	EL O/L Sin Res. Sight to Current Error
EL Sinusoidal Res	57	2	2	10	-	1° sin,	0. - 100Hz	EL Tach & Pos Fdbk	EL O/L Sin Res. Sight to Rate Loop Error
EL Sinusoidal Res	58	2	2	6	-	1° sin,	0. - 100Hz	EL Tach & Pos Fdbk	EL O/L Sin Res. Demodulator
EL Sinusoidal Res	59	2	10	14	-	1° sin,	0.1-100Hz	EL Tach & Pos Fdbk	EL O/L Sin Res. Rate & Current Loops
EL DC Gain	60	6	-	-	6, 8, 12, 14	2.0 VDC		EL Motor	EL Open Loop Gain, Input to Filter

Table A-1. Test and Input Point Identification

NUMBER	DESCRIPTION	LOCATION
1	Sight Stator, AZ	Sight Sim.
2	Sight Stator, EL	Sight Sim.
3	Demodulator Input, AZ	A1TP4
4	Demodulator Input, EL	A1TP5
5	Notch Filter Input, AZ	A1TP3
6	Notch Filter Input, EL	A1TP2
7	Notch Filter Output, AZ	A2R80
8	Notch Filter Output, EL	A2R104
9	Rate Loop Error Signal, AZ	A4R3, A4R8
10	Rate Loop Error Signal, EL	A3R3, A3R7
11	Current Loop Error Signal, AZ	A4R11, A4R12
12	Current Loop Error Signal, EL	A3R11, A3R12
13	Current Loop Amplifier Output, AZ	A4TP3
14	Current Loop Amplifier Output, EL	A3TP3
15	Motor Voltage, AZ	J4-F, J4-D
16	Motor Voltage, EL	J4-A, J4-C
17	Motor Current, AZ	J4-E (shunt)
18	Motor Current, EL	J4-B (shunt)
19	Tachometer Input, AZ	J3-R
20	Tachometer Input, EL	J3-T

NOTE: Other than the sight simulator, all locations are in the Turret Control assembly.

APPENDIX B

TESTS PERFORMED

UTS TEST NO.	TEST TYPE	TEST PLAN NO.	ITEMS DISCONNECTED	DESCRIPTION	NOTES
1	2° Elev Step	49	---	Elevation closed loop test	Limited data taken, preliminary test. Tests 1-13 were run in order to obtain quick data that could be used for preliminary analysis. The preliminary tests in the test plan will be run again later taking all data specified in the test plan. There is no real time data for test No. 6 due to A/D swap.
2	5° Elev Step	50	---	Elevation closed loop test	
3	10° Elev Step	--	---	Elevation closed loop test	
4	1°/Sec El ramp	--	---	EL ramp test (closed loop)	
5	2.5°/Sec El ramp	--	---	EL ramp test (closed loop)	
6	5°/Sec El ramp	--	---	EL ramp test (closed loop)	
7	5°/Sec El ramp	--	---	EL ramp test (closed loop)	
8	2° Azim Step	19	---	AZ step closed loop test	
9	5° Azim Step	20	---	AZ step closed loop test	
10	10° Azim Step	--	---	AZ step closed loop test	
11	1°/Sec AZ ramp	--	---	AZ ramp test (closed loop)	
12	2.5°/Sec AZ ramp	--	---	AZ ramp test (closed loop)	
13	5°/Sec AZ ramp	--	---	AZ ramp test (closed loop)	
14	AZ Sinusoid Resp	10-X1	AZ Motor	AZ O/L Sin Resp, Notch Filter	Special test Pts: Input: A2P1- ; Output: A2R71, AC213
15	AZ Sinusoid Resp	10	AZ Motor	AZ O/L Sin Resp, Notch Filter	No saturation evident, Input = .5V O-P

UTS TEST NO.	TEST TYPE	TEST PLAN NO.	ITEMS DISCONNECTED	DESCRIPTION	NOTES
16	AZ Sinusoid Resp	10-X2	AZ Motor	AZ O/L Sin Resp, Notch Filter	Special Output Test point: A2R71, A2C13, Input=.44 O-P
17	AZ Sinusoid Resp	11-1	AZ Motor	AZ O/L Sin Resp, Current Loop Amp	Input level caused saturation, Input = 1^{o}
18	AZ Sinusoid Resp	8-1	AZ Motor	AZ O/L Sin Resp; Forward Path to motor	Input level caused saturation, Input = 1^{o}.
19	AZ Sinusoid Resp	9	AZ Motor	AZ O/L Sin Resp For. Path to motor	Input level caused saturation, Input = 1^{o}.
20	EL Sinusoid Resp	39	EL Motor	EL O/L Sin Resp, For. Path to NOtch Filter	No saturation evident, Input = 1^{o}.
21	EL Sinusoid Resp	40	EL Motor	EL O.L Sin Resp Notch Filter	No saturation evident, Input = 1^{o}.
22	EL Sinusoid Resp	41-1	EL Motor	EL O/L Sin Resp Current Loop Amp	Input level caused saturation, Input = 1^{o}.
23	EL Sinusois Resp	38-1	EL Motor	EL O/L Sin Resp, Forward Path to motor	Input level caused saturation, Input = 1^{o}.
24	EL Sinusoid Resp	38-1A	EL Motor	EL O/L Sin Resp, Forward Path to motor	Rerun of previous to confirm results.
25	AZ Sinusoid Resp	8-2	AZ Motor	AZ O/L Sin Resp, Forward Path to motor	No saturation, Input level = 20MV P-P
26	AZ Sinusoid Resp	11-2	AZ Motor	AZ O/L Sin Resp, Current Loop Amp	Saturation, Input level = 20MV P-P
27	AZ Sinusoid Resp	11-3	AZ Motor	AZ O/L Sin Resp, Current Loop Amp	No saturation, Input level = 20MV P-P

UTS TEST NO.	TEST TYPE	TEST PLAN NO.	ITEMS DISCONNECTED	DESCRIPTION	NOTES
28	EL Sinusoid Resp	41-2	EL Motor	EL O/L Sin Resp, Current Loop Amp	No saturation, Input level = 20MV P-P
29	EL Sinusoid Resp	38-2	EL Motor	EL O/L Sin Resp, Forward Path to motor	No saturation, Input level = 20MV P-P
30	EL Sinusoid Resp	51-1	---	1^{o} EL C/L Sin Resp System	Response = $1/1 + G_{fp}$, G_{fp} = Path Gain
31	EL Sinusoid Resp	53-1	---	1^{o} EL C/L Sin Resp, Torq Dist Simul	Resp = (Demod Input)/ (Current Loop Error)
32	EL Sinusoid Resp	51-2	---	2.5^{o} EL C/L Sin Resp System	Response = $1/1\ G_{fp}$
33	EL Sinusoid Resp	52-1	---	2.5^{o} EL Sin Resp, Forward path	Resp = (Tach Input)/ (Sight Input)
34	EL Sinusoid Resp	54-1	---	1^{o} EL C/L Sin Resp, Torq Dist and Filter	Resp = (Notch Filter Output)/ (Current Loop Error)
35	EL Sinusoid Resp	55-1	---	1^{o} EL C/L Sin Resp, Torq Dist Forward path	Resp = (Tach Input)/ (Current Loop Error)
36	EL Sinusoid Resp	52-2	---	1^{o} EL C/L Sin Resp, Forward path	Resp = (Tach Input)/ (Sight Input)
37	EL Sinusoid Resp	53-2	---	2.5^{o} EL C/L Sin Resp, Torq Dist Simul	Resp = (Demod Input)/ (Current Loop Error)
38	EL Sinusoid Resp	53-3	---	0.5^{o} EL C/L Sin Resp, Torq Dist Simul	Resp = same as test 37
39	EL Sinusoid Resp	54-2	---	2.5^{o} EL C/L Sin Resp, Torq Dist and Filter	Resp = (Notch Filter Output)/ (Current Loop Error)

UTS TEST NO.	TEST TYPE	TEST PLAN NO.	ITEMS DISCONNECTED	DESCRIPTION	NOTES
40	EL Sinusoid Resp	54-2A	---	2.5° EL C/L Sin Resp, Torq Dist and Filter	Resp same as test 39, Rerun of 39 for smoother data
41	EL Sinusoid Resp	54-3	---	0.5° EL C/L Sin Resp, Torq Dist and Filter	Resp same as test 39
42	EL Sinusoid Resp	55-2	---	2.5° EL C/L Sin Resp, Torq Dist For. Path	Resp = (Tach Input)/(Current Loop Error)
43	EL Sinusoid Resp	55-3	---	0.5° EL C/L Sin Resp Torq Dist For Path	Resp Same as test 42
44	AZ Sinusoid Resp	25-3	---	0.5° AZ C/L Sin Resp, Torq Dist For. Path	Resp = (Tach Input)/(Current Loop Error)
45	AZ Sinusoid Resp	25-2	---	1° AZ C/L Sin Resp, Torq Dist For. Path	Resp same as test 44.
46	AZ Sinusoid Resp	25-1	---	2.5° AZ C/L Sin Resp, Torq Dist For. Path	Resp same as test 44.
47	AZ Sinusoid Resp	24-1	---	2.5° AZ C/L Sin Resp, Torq Dist and Filter	Resp = (Notch Filter Output)/ (Current Loop Error)
48	AZ Sinusoid Resp	24-2	---	1° AZ C/L Sin Resp, Torq Dist and Filter	Resp same as test 47
49	AZ Sinusoid Resp	24-3	---	0.5° AZ C/L Sin Resp, Torq Dist and Filter	Resp same as test 47
50	AZ Sinusoid Resp	23-3	---	0.5° AZ C/L Sin Resp, Torq Dist Simul.	Resp = (Demod Input)/ Current Loop Error
51	AZ Sinusoid Resp	23-2	---	1° AZ C/L Sin Resp, Torq Dist Simul.	Resp same as test 50

UTS TEST NO.	TEST TYPE	TEST PLAN NO.	ITEMS DISCONNECTED	DESCRIPTION	NOTES
52	AZ Sinusoid Resp	23-1	---	2.5° AZ C/L Sin Resp Tor Dist Simul	Resp same as test 50
53	AZ Sinusoid Resp	22-1	---	2.5° AZ C/L Sin Resp, Forward path	Resp = (Tach Input)/(Sight Input)
54	AZ Sinusoid Resp	22-2	---	1° AZ C/L Sin Resp, Forward path	Resp same as test 53
55	AZ Sinusoid Resp	22-3	---	0.5° AZ C/L Sin Resp, Forward path	Resp same as test 53
56	AZ Sinusoid Resp	21-3	---	0.5° AZ C/L Sin Resp System	Resp = $1/1 + G_{fp}$
57	AZ Sinusoid Resp	21-2	---	1° AZ C/L Sin Resp System	Response same as test 56
58	AZ Sinusoid Resp	21-1	---	2.5° AZ C/L Sin Resp System	Response same as test 56
59	AZ Sinusoid Resp	16	AZ Position FDBK	AZ O/L Sin Resp, rate loop	Resp = (Rate Loop Error)/(Notch Filter Output) Input = .2V 0 to peak
60	AZ Sinusoid Resp	14	AZ Tach & Pos FDBK	1° AZ O/L Sin Resp, Sight to Current Out	Resp = (Current Loop Amp)/(Sight Input)
61	AZ Sinusoid Resp	12	AZ Tach & Pos FDBK	1° AZ O/L Sin Resp, Current Loop	Resp = (Current Loop Error)/(Current Loop Output)
62	AZ Sinusoid Resp	14-A	AZ Tach & Pos FDBK	1° AZ O/L Sin Resp, Sight to Current Out	Rerun of test 60
63	AZ Sinusoid Resp	7	AZ Tach & Pos FDBK	1° AZ O/L Sin Resp Forward path	Resp = (Notch Filter Output)/(Sight Input)
64	AZ Sinusoid Resp	13	AZ Tach & Pos FDBK	1° AZ O/L Sin Resp, motor Loop Fwd Path	Resp = (Tach Input)/(Current Loop Output)

UTS TEST NO.	TEST TYPE	TEST PLAN NO.	ITEMS DISCONNECTED	DESCRIPTION	NOTES
65	EL Sinusoid Resp	37	EL Tach & Pos FDBK	1^{o} EL O/L Sin Resp Forward path	Resp = (Notch Filter Output)/ (Sight Input)
66	EL Sinusoid Resp	43	EL Tach & Pos FDBK	1^{o} EL O/L Sin Resp, motor loop fwd path	Resp = (Tach Input)/(Current Loop Output)
67	EL Sinusoid Resp	44	EL Tach & Pos FDBK	1^{o} EL O/L Sin Resp, sight to current Out.	Resp = (Current Loop Amp)/ (Sight Input)
68	EL Sinusoid Resp	45	EL Tach & Pos FDBK	1^{o} EL O/L Sin Resp, Fwd path to Tach	Resp = (Tach Input)/(Notch Filter Output)
69	EL Sinusoid Resp	56	EL Tach & Pos FDBK	1^{o} EL O/L Sin Resp, Sight to Current Error	Resp = (Current Loop Error)/ (Sight Input)
70	EL Sinusoid Resp	57	EL Tach & Pos FDBK	1^{o} EL O/L Sin Resp, Sight to Rate Loop Error	Resp = (Rate Loop Error)/ (Sight Input)
71	EL Sinusoid Resp	58	EL Tach & Pos FDBK	1^{o} EL O/L Sin Resp, Demodulator	Resp = (Notch Filter Input)/ (Sight Input)
72	EL Sinusoid Resp	59	EL Tach & Pos FDBK	1^{o} EL O/L Sin Resp, Rate & Current Amps	Resp = (Current Loop Output)/ (Rate Loop Error)
73	EL Sinusoid Resp	46	EL Position FDBK	1^{o} EL O/L Sin Resp, Rate Loop	Resp = (Rate Loop Error)/ (Notch Filter Output)
74	AZ Sinusoid Resp	26	AZ Tach & Pos FDBK	1^{o} AZ O/L Sin Resp, sight to current error	Resp = (Current Loop Error)/ (Sight Input)
75	AZ Sinusoid Resp	27	AZ Tach & Pos FDBK	1^{o} AZ O/L Sin Resp, sight to rate error	Resp = (Rate Loop Error)/ (Sight Input)
76	AZ Sinusoid Resp	28	AZ Tach & Pos FDBK	1^{o} AZ O/L Sin Resp, demodulator	Resp = (Notch Filter Input)/ (Sight Input)

UTS TEST NO.	TEST TYPE	TEST PLAN NO.	ITEMS DISCONNECTED	DESCRIPTION	NOTES
77	AZ Sinusoid Resp	29	AZ Tach & Pos FDBK	1° AZ O/L Sin Resp, Rate & Current Amps	Resp = (Current Loop Output)/ (Rate Loop Error)
78	AZ Sinusoid Resp	15	AZ Tach & Pos FDBK	1° AZ O/L Sin Resp, Forward Path to Tach	Resp = (Tach Input)/ (Current Loop Output)
79	AZ Step Response	4-1	Azimuth Motor	2° AZ O/L Step Response	The output was saturated for tests 79-83
80	AZ Step Response	4-2	Azimuth Motor	1° AZ O/L Step Response	
81	AZ Step Response	4-3	Azimuth Motor	0.5° AZ O/L Step Response	No real data due to A/D swap
82	AZ Step Response	4-3A	Azimuth Motor	0.5° AZ O/L Step Response	Rerun of test 81
83	AZ Step Response	4-4	Azimuth Motor	0.25° AZ O/L Step Response	
84	AZ Step Response	4-5	Azimuth Motor	0.12° AZ O/L Step Response	No saturation evident in output
85	AZ Step Response	19	---	1° Azimuth Closed Loop Resp	Data for tests 85 and 86 were not satisfactory
86	AZ Step Response	20	---	2.5° Azimuth Closed Loop Response	
87	AZ Step Response	20-A	---	2.5° Azimuth Closed Loop Response	Rerun of test 86
88	AZ Step Response	19-A	---	1° Azimuth Closed Loop Response	Rerun of test 85
89	AZ DC Gain	1	Azimuth Motor	Azimuth DC Open Loop Gain	Input = 2.0 VDC Demodulator Error

UTS TEST NO.	TEST TYPE	TEST PLAN NO.	ITEMS DISCONNECTED	DESCRIPTION	NOTES
90	AZ Step Response	5	Azimuth Motor	AZ O/L Step Resp, Input to Notch Filter	Very little response seen, Loading problem
91	AZ Step Response	3	AZ Tach & Pos FDBK	1^{o} AZ Open Loop Step Response	Data Channel Saturated
92	AZ Step Response	3-A	AZ Tach & Pos FDBK	1^{o} AZ Open Loop Step Response	Rerun of test 91
93	AZ Open Loop Res	17	AZ Tach & Pos FDBK	AZ O/L Res, Minimum Input for Motion	Turret touched mechanical stop
94	AZ Open Loop Res	17-A	AZ Tach & Pos FDBK	AZ O/L Res, Minimum Input for motion	Input = $\pm$.7MR Step, Repeat of test 93
95	AZ Open Loop Res	18	AZ Tach & Pos FDBK	2.5^{o} AZ Open Loop Response	
96	EL Step Response	34-1	Elevation Motor	2^{o} EL O/L Step Response	
97	EL Step Response	34-2	Elevation Motor	1^{o} EL O/L Step Response	
98	EL Step Response	34-3	Elevation Motor	0.5^{o} EL O/L Step Response	
99	EL Step Response	34-4	Elevation Motor	0.25^{o} EL O/L Step Response	
100	EL Step Response	34-5	Elevation Motor	0.12^{o} EL O/L Step Response	
101	EL DC Gain	31	Elevation Motor	Elevation DC Open Loop Gain	
102	EL Step Response	33	EL Tach & Pos FDBK	1^{o} EL Open Loop Step Response	Data Channels Disconnected
103	EL Open Loop Resp	48	EL Tach & Pos FDBK	2.5^{o} EL Open Loop Response	Data Channels Disconnected
104	EL Open Loop Resp	48-A	EL Tach & Pos FDBK	2.5^{o} EL Open Loop Response	Rerun of test 103
105	EL Open Loop Resp	47	EL Tach & Pos FDBK	EL O/L Res, Minimum Input for motion	Input = $\pm$.7MR step

UTS TEST NO.	TEST TYPE	TEST PLAN NO.	ITEMS DISCONNECTED	DISCONNECTED	NOTES
106	EL Step Response	33-A	EL Tach & Pos FDBK	1^{o} EL Open Loop Response	Rerun of test 102
107	EL Step Response	49	---	1^{o} Elevation Closed Loop Response	
108	EL Step Response	50	---	2.5^{o} Elevation Closed Loop response	
109	Azimuth Backlash	Para 2.2	---	Measurement of gear backlash	8 measurements were taken and averaged in each test 109-110
110	Elevation Backlash	Para 2.2	---	Measurement of gear backlash	

APPENDIX C

THEORETICAL DERIVATION OF NOTCH FILTER TRANSFER FUNCTION

In order to obtain a validated mathematical model for the notch filter circuits, their theoretical transfer function was derived and the response of this model was compared to the experimental results. The transfer function had to be derived for the same circuitry whose response was experimentally measured. This circuit is shown in Figure C-1.

The transfer function is derived in two parts. First, the transfer function for e_0/e_A is calculated as $\frac{e_0}{e_A} = \frac{R_6+R_5}{R_5} = \frac{108.8}{2} = 54.4$, assuming that the input current to AR1 is zero. Second, the transfer function e_A/e_i is calculated using four loop equations:

$$\begin{bmatrix} R_i + \frac{1}{SC_1} & -\frac{1}{SC_1} & -R_1 & 0 \\ -\frac{1}{SC_1} & R_2 + \frac{1}{SC_1} + \frac{1}{SC_2} & -\frac{1}{SC_2} & 0 \\ -R_1 & -\frac{1}{SC_2} & R_1 + R_3 + \frac{1}{SC_2} + \frac{1}{SC_3} & -\frac{1}{SC_3} \\ 0 & 0 & -\frac{1}{SC_3} & R_4 + \frac{1}{SC_3} \end{bmatrix} \quad X$$

$$\begin{bmatrix} I_1 \\ I_2 \\ I_3 \\ I_4 \end{bmatrix} = \begin{bmatrix} e_i \\ 0 \\ 0 \\ 0 \end{bmatrix}$$

These equations are used to solve for I_4 in terms of e_i. Then e_A/e_i is found using the relation $e_A = I_4/R_4$. Finally, e_o/e_i is found by multiplying:

$$\frac{e_A}{e_I} \times \frac{e_o}{e_A} = \frac{R_6+R_5}{R_5} \quad \frac{e_A}{e_I} = \frac{e_o}{e_i} .$$

Following the outlined steps, this transfer function is derived:

$$\frac{e_o}{e_i} = \frac{G(N_2S^2 + N_1S + N_0)}{D_3S^3 + D_2S^2 + D_1S + D_0}$$

where the gain, G, is: $\frac{R_6+R_5}{R_5}$, and the coefficient terms are:

$$N_2 = R_1R_2C_1C_2$$

$$N_1 = R_1C_2+R_1C_1$$

$$N_0 = 1$$

$$D_3 = R_1R_2R_3C_1C_2C_3$$

$$D_2 = R_1R_2C_1C_2 + R_1R_3C_1C_3 + R_1R_2C_2C_3 + R_2R_3C_2C_3 + R_1R_3C_2C_3 + \frac{R_1R_2R_3C_1C_2}{R_4}$$

$$D_1 = R_1C_2 + R_2C_2 + R_1C_1 + R_2C_3 + \frac{R_1R_3C_1}{R_4} + \frac{R_1R_2C_1}{R_4} + \frac{R_1R_2C_2}{R_4} + \frac{R_2R_3C_2}{R_4} + R_3C_3$$

$$D_0 = 1 + \frac{R_2}{R_4} + \frac{R_3}{R_4}$$

When the following component values:

R_1	= 1000 ohms	R_5	= 2000 ohms
R_2	= 20000 ohms (elevation)	R_6	= 106800 ohms
R_2	= 26100 ohms (azimuth)	C_1	= 10 microfarads
R_3	= 1900 ohms	C_2	= 1.5 microfarads
R_4	= 2000 ohms	C_3	= 4.7 microfarads

are substituted into the theoretical transfer function, two numerical transfer functions are obtained:

(1) azimuth:

$$\frac{e_o}{e_i} = 54.4 \left[\frac{(3.915 \times 10^{-4})S^2 + (1.15 \times 10^{-2})S + 1}{(3.496 \times 10^{-6})S^3 + (2.626 \times 10^{-3})S^2 + (3.802 \times 10^{-1})S + 15} \right]$$

(2) elevation:

$$\frac{e_o}{e_i} = 54.4 \left[\frac{(3.0 \times 10^{-4})S^2 + (1.15 \times 10^{-2})S + 1}{(2.679 \times 10^{-6})S^3 + (2.036 \times 10^{-3})S^2 + (2.989 \times 10^{-1})S + 11.95} \right]$$

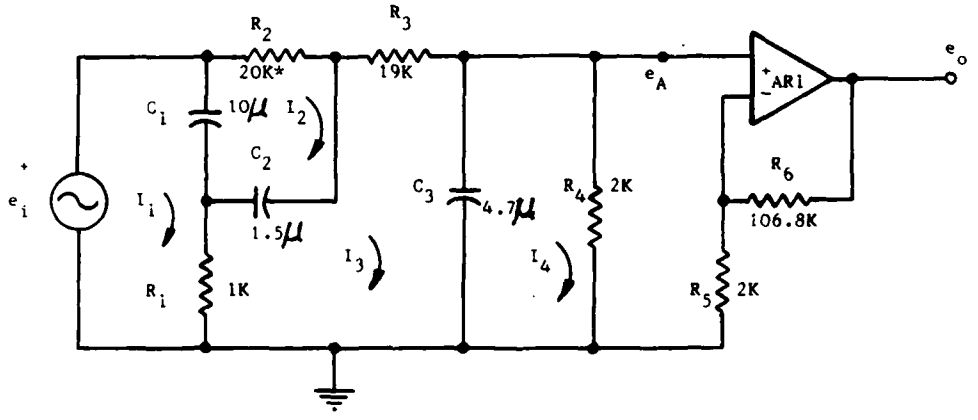

*R_2 = 20K for Elevation and 26.1K for Azimuth

Figure derived from drawing 11830588

FIGURE C-1 NOTCH FILTER CIRCUIT DIAGRAM

APPENDIX D

STATISTICAL ANALYSIS OF FIRING DATA

The target impact points of each round were first analyzed to determine the standard deviation of the shot group of each of the three barrels of the M197 gun for each test. The first three rounds of each burst were not included in the analysis. Thus, the standard deviations for the first barrel fired were calculated from the impact points of rounds 4, 7, 10, 13, 16, and 19. Similarly, rounds 5, 8, 11, 14, 17, and 20 were used to calculate the dispersion of the second barrel fired, and rounds 6, 9, 12, 15, and 18 were used for the third.

Standard deviations for each barrel were calculated using the equation

$$S = \frac{\sum_{i=1}^{n} (X_i - \overline{X})^2}{n-1} \qquad \text{D-1}$$

where the X_i represents the distance of the impact point in inches from the point-of-aim (POA), n = number of rounds from the barrel, and $\overline{X}$ = mean of barrel group = $\frac{\sum_{i=1}^{n} X_i}{n}$

Standard deviations were calculated for each barrel in both elevation and azimuth. In elevation, X is the vertical distance from the POA to the impact point; and in azimuth, X is the horizontal distance.

An example of the test data from which the standard deviations were calculated is shown in table D-1. As an example, the standard deviation in azimuth for the first barrel fired in test 84 is calculated as follows:

First, $\overline{X} = \frac{1}{6}((-5.8) + (-5.4) + (-5.2) + (-3.2) + (-5.3)) = -5.117$

then, $S = \frac{1}{5}[(-5.8 - (-5.117))^2 + (-5.4 - (-5.117))^2 + (-5.2 - (-5.117))^2$

$+ (-5.8 - (-5.117))^2 + (-3.2 - (5.117))^2 + (-5.3 - (-5.117))^2] = 0.97$

The standard deviations are summarized in tables D-2 and D-3. The mean and standard deviations of these standard deviations shown at the bottom of these tables were calculated by use of equation D-1.

A statistical analysis can be carried out on the data shown in tables D-2 and D-3 to obtain more information about the tested controller and turret performance. First, an analysis of variance technique can be used to determine if the type of controller used has a statistically significant effect on the shot dispersion and, further, if any statistical difference exists in the standard deviations of a barrel depending on whether it is fired first, second, or third.

Further information on the statistical techniques used in this appendix can be found in references D-1 and D-2. The first step in the analysis is to organize the data into a table and make the preliminary calculations. This step is shown in table D-4 for azimuth and in table D-5 for elevation.

Table D-1. Firing test data for test 84

Round	Impact distance from point-of-aim (POA)* (in.) AZ	EL
1	-0.8	1.9
2	-2.4	5.1
3	-4.5	1.2
4	-5.8	-4.9
5	-2.6	-7.4
6	-4.4	-5.8
7	-5.4	-7.3
8	-2.3	-4.4
9	-3.9	-1.3
10	-5.2	-3.7
11	-3.5	-4.2
12	-4.2	-2.2
13	-5.8	-5.7
14	-5.0	-2.6
15	-3.9	-1.7
16	-3.2	-4.5
17	-1.6	-4.4
18	-4.2	-3.6
19	-5.3	-6.8
20	-3.3	-5.2

* POA is the point to which the weapon is boresighted before the test. Positive numbers indicate impact to the right of the POA in azimuth and above the POA in elevation.

Table D-2. Firing test standard deviations for XM97 program

Test no.	Standard deviation (mr) Rounds 4,7,10,13,16,19 AZ	EL	Rounds 5,8,11,14,17,20 AZ	EL	Rounds 6,9,12,15,18 AZ	EL
188	1.00	2.45	1.40	1.19	2.30	1.54
189	1.88*	2.09*	1.54*	0.66*	1.31*	1.86*
190	0.92	1.02	1.31	1.05	1.67	0.46
191	1.79	1.69	2.51	2.68	1.19	2.25
199	1.10	2.12	1.58	3.38	1.68	0.76
200	0.76	1.53	0.85	2.01	0.75	1.50
205	1.69	2.56	1.69	2.63	1.96	1.50
226	0.89	1.73	1.06	2.85	0.85	2.59
258	1.14*	6.70*	2.17*	4.06*	2.16*	2.24*
269	0.65	2.84	0.82	2.96	0.59	2.38
270	0.57	1.71	0.64	1.89	0.78	1.60
273	1.20	2.33	1.24	2.22	1.69	0.90
274	1.09	2.36	1.23	1.56	1.17	1.33
275	1.56	1.45	2.43	1.54	1.62	2.82
276	1.31*	2.65*	1.02*	2.41*	1.08*	2.13*
277	0.66*	4.16*	0.95*	3.78*	0.71*	3.18*
Optim mean	1.10	1.98	1.40	2.16	1.35	1.64
Optim std dev	0.40	0.54	0.59	0.75	0.54	0.74
Orig mean	1.25	3.90	1.42	2.73	1.32	2.36
Orig std dev	0.50	2.06	0.57	1.56	0.62	0.57

* Original system in control.

Table D-3. Firing test standard deviations for UTS program

Test no.	Standard deviation (mr)					
	Rounds 4,7,10,13,16,19		Rounds 5,8,11,14,17,20		Rounds 6,9,12,15,18	
	AZ	EL	AZ	EL	AZ	EL
79	0.76*	1.43	1.65*	1.54	0.57*	2.22
80	1.08*	1.56	0.73*	1.00	1.01*	1.21
81	0.83	1.71*	0.71	2.69*	0.70	1.81*
82	2.43	2.32*	0.91	0.88*	0.57	1.49*
84	0.97	1.38*	1.18	1.57*	0.22	1.83*
85	0.74*	0.95*	0.61*	0.88*	0.73*	1.50*
86	1.11*	1.44*	2.49*	1.05*	0.82*	1.08*
87	1.48*	1.93*	1.23*	1.28*	0.72*	2.17*
94	0.75	1.23	0.59	1.13	1.02	2.47
95	0.57	1.89	0.53	1.63	1.17	1.66
96	0.71	1.37	0.67	1.20	0.70	1.60
97	1.04	1.40	0.34	1.66	0.36	1.12
98	0.49	1.80	0.40	1.84	0.42	1.95
Optim mean	0.97	1.53	0.67	1.43	0.64	1.75
Optim std dev	0.62	0.24	0.27	0.32	0.33	0.50
Orig mean	1.03	1.62	1.34	1.39	0.77	1.65
Orig std dev	0.30	0.48	0.76	0.69	1.16	0.37

* Original system in control.

Table D-4. Azimuth data table and preliminary calculations

System	Barrel firing number*				
	First	Second	Third	$T_{i\cdot}$	$T_{i\cdot}^2$
Original XM97	1.25	1.42	1.32	3.99	15.9201
Optimal XM97	1.10	1.40	1.35	3.85	14.8225
Original UTS	1.03	1.34	0.77	3.14	9.8596
Optimal UTS	0.97	0.67	0.64	2.28	5.1984
$T_{\cdot j}$	4.35	4.83	4.08		
$T_{\cdot j}^2$	18.9225	23.3289	16.6464		

$T_{\cdot\cdot} = 13.26$

$$\sum_{i=1}^{4} T_{i\cdot}^2 = 45.8006$$

$$\sum_{j=1}^{3} T_{\cdot j}^2 = 58.8978$$

$T_{\cdot\cdot}^2 = 175.8276$

$$\sum_{i=1}^{4} \sum_{j=1}^{3} X_{ij}^2 = 15.5626$$

---

* The "T" notation is shorthand for row and column summation, that is,

$$T_{i\cdot} = \sum_{j=1}^{3} X_{ij},\ T_{\cdot j} = \sum_{i=1}^{4} X_{ij},\ \text{and}\ T_{\cdot\cdot} = \sum_{i=1}^{4} \sum_{j=1}^{3} X_{ij}.$$

Table D-5. Elevation data table and preliminary calculations

System	Barrel firing number* First	Second	Third	$T_{i\cdot}$	$T_{i\cdot}^2$
Original XM97	3.90	2.73	2.36	8.99	80.8201
Optimal XM97	1.98	2.16	1.64	5.78	33.4084
Original UTS	1.62	1.39	1.65	4.66	22.1841
Optimal UTS	1.53	1.43	1.75	4.71	21.7156
$T_{\cdot j}$	9.03	7.71	7.40		
$T_{\cdot j}^2$	81.5409	59.4441	54.76		

$T_{\cdot\cdot} = 24.14$ $\quad T_{\cdot\cdot}^2 = 582.7396$ $\quad \sum_{i=1}^{4} T_{i\cdot}^2 = 158.1282$

$\sum_{j=1}^{3} T_{\cdot j}^2 = 195.745$ $\quad \sum_{i=1}^{4} \sum_{j=1}^{3} X_{ij}^2 = 54.2354$

---

* The "T" notation is shorthand for row and column summation, that is,

$$T_{i\cdot} = \sum_{j=1}^{3} X_{ij},\ T_{\cdot j} = \sum_{i=1}^{4} X_{ij},\ \text{and}\ T_{\cdot\cdot} = \sum_{i=1}^{4} \sum_{j=1}^{3} X_{ij}.$$

The data in tables D-4 and D-5 is used to test two hypotheses. The first hypothesis is that the means of the data for the systems are equal. Notationally this idea is stated as:

$H_o : \mu_{\text{Original XM97}} = \mu_{\text{Optimal XM97}} = \mu_{\text{Original UTS}} = \mu_{\text{Optimal UTS}}$.

This approach also can be interpreted as stating that the system used has no effect on the shot dispersion. The second hypothesis is that the means of the data for the barrel firing numbers are equal, or $H_o : \mu_1 = \mu_2 = \mu_3$. This approach also means, if true, that the moment when the barrel is fired has no effect on the shot dispersion of that barrel. The alternative to each hypothesis is that at least two of the means differ.

Acceptance or rejection of each hypothesis is based on calculations made of the data. In each case, a test statistic is determined for the mean square of

the data and is compared with a critical statistic obtained from a table. If the test statistic is greater than the critical statistic, then the hypothesis is rejected. The test statistic for the systems hypothesis is calculated by

$$F = \frac{MS_{system}}{MS_{error}} = \frac{SS_{system/3}}{SS_{error/6}} \qquad D\text{-}2$$

where

$$SS_{system} = \text{Sum of squares (system)} = \frac{\sum_{i=1}^{4} T_i^2}{3} - \frac{T_{..}^2}{12} \qquad D\text{-}3$$

$$SS_{error} = \text{Sum of squares (error)} = \sum_{i=1}^{4}\sum_{j=1}^{3} X_{ij}^2 - \sum_{i=1}^{4} \frac{Ti.^2}{3} - \sum_{j=1}^{3} \frac{T.j^2}{3} + \frac{T_{..}^2}{12} \qquad D\text{-}4$$

In a like manner, the test statistic for the barrel hypothesis is calculated by

$$F = \frac{MS_{barrel}}{MS_{error}} = \frac{SS_{barrel}/2}{SS_{error}/6} \qquad D\text{-}5$$

where

$$SS_{barrel} = \text{Sum of squares (barrel)} = \frac{\sum_{j=1}^{3} T.j^2}{4} - \frac{T_{..}^2}{12} \qquad D\text{-}6$$

SS_{error} is calculated by use of equation D-4.

The calculations are summarized in an Analysis of Variance (ANOVA) table. The ANOVA tables for azimuth and elevation are shown in table D-6.

Table D-6. ANOVA tables—system and barrel effects considered

Source	Sum of squares	Degree of* freedom	MS	F	$F_{critical}$
		AZIMUTH			
System	0.61457	3	0.20486	5.4981	3.2888
Barrel	0.07215	2	0.03608	0.9683	3.4633
Error	0.22358	6	0.03726		
Total	0.91030	11			
		ELEVATION			
System	4.14777	3	1.38259	7.20474	3.2888
Barrel	0.37462	2	0.18731	0.97608	3.4633
Error	1.15138	6	0.19190		
Total	5.67377	11			

* One less than number of data points used to calculate a given mean.

Since the degrees of freedom is equal to one less than the number of data points used to calculate a given mean, $df_{error} = df_{system} \times df_{barrel}$. The critical statistic $F_{critical}$ is obtained from a standard table of F statistics. The value of $F_{critical}$ depends on the degrees of freedom of the mean squares involved and the level of confidence, α, chosen for the analysis. A α value of 0.10, which corresponds to having 90% confidence in the results, was chosen.

Then, $F_{critical, systems} = F_{\alpha, (df_{systems}, df_{error})} = F_{0.10(3,6)} = 3.2888$

and $F_{critical, barrel} = F_{\alpha, (df_{barrel}, df_{error})} = F_{0.10(2,6)} = 3.4633$

According to the theory, the hypothesis can be rejected if $F > F_{critical}$. The ANOVA tables show that for both azimuth and elevation the hypothesis about the system means can be rejected, but that the hypothesis about the barrel means cannot be rejected. This approach indicates that at least two of the means of the firing data standard deviations for the different systems are different. Further, then, this idea is an indication that the type of system used to control the turret does affect the shot dispersion. On the other hand, the data also

shows that whether a barrel is fired first, second, or third in a burst makes no difference in the shot dispersion.

Since at least two of the system means differ, more information can be determined by application of the most-significant-difference (MSD) test. Also known as the multiple-t test, this method is used to determine which data means are different in a statistically significant manner. While the data summary in tables D-4 and D-5, show that the standard deviation means are smaller for the optimal and UTS systems, the MSD method will tell if the differences can be called significant within a confidence level of 90%.

Before the MSD method can be applied, ANOVA tables must be calculated wherein the barrel firing number is not taken into account. These ANOVA tables are shown in table D-7.

Table D-7. ANOVA tables--barrel effects ignored

Source	Sum of squares	Degree of* freedom	MS	F	$F_{critical}$
		AZIMUTH			
System	0.61457	3	0.20486	5.5412	2.9238
Error	0.29573	8	0.03697		
Total	0.91030	11			
		ELEVATION			
System	4.14777	3	1.38259	7.2482	2.9238
Error	1.52600	8	0.19075		
Total	5.67377	11			

* One less than number of data points used to calculate a given mean.

These ANOVA tables indicate that the system means are not all equal. The MSD method requires the MS_{error} term from the tables to calculate the standard error of the mean, $S_{\bar{x}}$:

$$S_{\bar{x}} = \sqrt{\frac{MS_E}{M}} \qquad \text{D-7}$$

where M is the number of data points involved in calculating the system means.

The standard errors of the mean for azimuth are: $S_{\bar{x}} = \sqrt{\frac{0.03697}{3}} = 0.1110$ and for elevation: $S_{\bar{x}} = \sqrt{\frac{0.19075}{3}} = 0.25658$. These numbers are used to calculate MSD number from the formula: $MSD = \sqrt{2}\, S_{\bar{x}}\, t_{0.10,8}$. D-8

The t-statistic is obtained from any standard statistics table. The numbers are:

Azimuth: $MSD = (\sqrt{2})\ (0.111)\ (1.397) = 0.219$

Elevation: $MSD = (\sqrt{2})\ (0.25658)\ (1.397) = 0.507$

Next tables of differences are set up wherein the means are calculated and sorted and the differences found. The process is illustrated in tables D-8 and D-9.

Table D-8. Azimuth mean ranking and differences tables

System	Test replications 1	2	3	Total	Mean
A: Original XM97	1.25	1.42	1.32	3.99	1.330
B: Optimal XM97	1.10	1.40	1.35	3.85	1.283
C: Original UTS	1.03	1.34	0.77	3.14	1.047
D: Original UTS	0.97	0.67	0.64	2.28	0.760

Mean Rank: Largest: System A
2nd Largest: System B
2nd Smallest: System C
Smallest: System D

	A 1.330	B 1.283	D 1.047
D: 0.760	0.570	0.523	0.287
C: 1.047	0.283	0.236	—
B: 1.283	0.047	—	—

Table D-9. Elevation mean ranking and differences tables

System	Test replications 1	2	3	Total	Mean
A: Original XM97	3.90	2.73	2.36	8.99	2.9967
B: Optimal XM97	1.98	2.16	1.64	5.78	1.9267
C: Original UTS	1.62	1.39	1.65	4.66	1.5533
D: Original UTS	1.53	1.43	1.75	4.71	1.5700

Mean Rank:
Largest: System A
2nd Largest: System B
2nd Smallest: System D
Smallest: System C

		A 2.9967	B 1.9267	D 1.5700
C:	1.5533	[1.4434]	0.3734	0.0167
D:	1.5700	[1.4267]	0.3567	--
B:	1.9267	[1.0700]	--	--

In the MSD method, the differences are compared to the MSD number calculated using equation D-8. Every difference in the table that exceeds MSD corresponds to two means that come from different populations; i.e., the means are different. Those differences exceeding MSD are circled in the figures. In table D-8 all differences are circled except B-A = 0.047. This indicates that there is no statistically significant difference between the performance of Systems A and B. However, there are statistically significant differences between all other system combinations, i.e., (A,D), (B,D), (C,D), (A,C), and (B,C). For elevation, from table D-9, there is no statistically significant difference between systems (B,C), (C,D), and (B,D), but there is between systems (A,C), (A,D), and (A,B).

Several conclusions can be drawn from the results of applying the MSD method. First, in azimuth, each UTS system performed significantly better than each XM97 system. In addition, the optimal UTS system performed significantly better than the original UTS system. However, the optimal XM97 controller did not show better performance than the original XM97 controller. In elevation, on the other hand, the optimal XM97 controller showed significant improvement over the original XM97 controller, but there is no difference between the performances of the original and optimal UTS controllers.

REFERENCES

D-1. C. R. Hicks, Fundamental Concepts in the Design of Experiments, second edition, Holt, Rinehart, and Winston, Inc., New york, 1973.

D-2. U.S. Army Managem nt Engineering Training Activity, Statistical Analysis and Design Experiments, Course Book, Defense Management Joint Course, Rock Island, IL 1979.

DISTRIBUTION LIST

Office of the Deputy Undersecretary
of Defense Research and Engineering
Pentagon Room 3D1098
Washington, DC 20301

Commander
U.S. Army Materiel Development
and Readiness Command
ATTN: DRCDE
DRCIRD
5001 Eisenhower Avenue
Alexandria, VA 22333

Commander
Combined Army Center
ATTN: ATCA-COF
Ft. Leavenworth, KS 66048

Commanding General
Training and Doctrine Command
ATTN: Library Bldg 133
Ft. Monroe, VA 23651

Commander
Army Tank Automotive Research
and Development Command
ATTN: DRDTA-UL, Library
Warren, MI 48090

Commandant
U.S. Army Aviation Center
P.O. Box O
ATTN: USAAVNT, Library
Ft. Rucker, AL 36362

Commander
Harry Diamond Laboratory
2800 Powder Mill Road
ATTN: DELHD-PP
Adelphi, MD 20783

Commander
U.S. Army Aviation Research
and Development Command
P.O.Box 209
ATTN: DRDAV-EVW
St. Louis, MO 63166

Program Manager
Fighting Vehicle Systems
MAMP Bldg 1
ATTN: DRCPM-FVS-SEA
Warren, MI 48090

Project Manager
Advanced Attack Helicopter
P.O. Box 209
ATTN: DRCPM-AAH
St. Louis, MO 63166

Administrator
Defense Technical Information Center
ATTN: Accessions Division (12)
Cameron Station
Alexandria, VA 22314

Director
U.S. Army Materiel Systems
Analysis Activity
ATTN: DRXSY-MP
Aberdeen Proving Ground, MD 21005

Commander
U.S. Army Armament Materiel
Readiness Command
ATTN: DRSAR-LE
DRSAR-LEP-L
Rock Island, IL 61299

Headquarters
U.S. Army Research and Technical Laboratory
Ames Research Center
ATTN: DAVDL-AS
Moffett Field, CA 94035

Commander
U.S. Army Armament Research
and Development Command
ATTN: DRDAR-TSE-SW (20)
Rock Island, IL 61299

Commander (Code 3176)
Naval Weapons Center
ATTN: Technical Library
China Lake, CA 03555

Department of the Navy (Code 5323D)
Naval Air Systems Command
ATTN: Technical Library
Washington, DC 20361

Commander (Code G22)
Naval Surface Weapons Center
ATTN: Technical Library
Dahlgren, VA 22448

Commander
Air Force Armament Laboratory
ATTN: Technical Library
Eglin Air Force Base, FL 32548

Commander/Director
Chemical Systems Laboratory
U.S. Army Armament Research
and Development Command
ATTN: DRDAR-CLJ-L
DRDAR-CLB-PA
APG, Edgewood Area, MD 21010

Director
Ballistics Research Laboratory
U.S. Army Armament Research
and Development Command
ATTN: DRDAR-TSB-S
Aberdeen Proving Ground, MD 21005

Chief
Benet Weapons Laboratory, LCWSL
U.S. Army Armament Research
and Development Command
ATTN: DRDAR-LCB-TL
Watervliet, NY 12189

Director
U.S. Army TRADOC Systems
Analysis Activity
ATTN: ATAA-SL
White Sands Missile Range, NM 88002

Director
Industrial Base Engineering Activity
ATTN: DRXIB-MT
Rock Island, IL 61299

Commandant
U.S. Army Aviation Center
ATTN: ATZQ-D-MS
P.O. Box 0
Ft. Rucker, AL 36362

Commander
U.S. Army Armament Research
and Development Command
ATTN: DRDAR-SCS-E
DRDAR-SCF-CC
DRDAR-SCS-M
DRDAR-TS
DRDAR-TSE
DRDAR-TSS (5)
DRDAR-GCL
Dover, NJ 07801

Commander
U.S. Army Aviation Research
and Development Command
ATTN: DRDAV-NS
4300 Goodfellow Blvd
St. Louis, MO 63120

Project Manager Cobra
ATTN: DRCPM-CO-TM
4300 Goodfellow Blvd
St. Louis, MO 63120